AGU PUBLICATIONS

Geochemistry, Geophysics, Geosystems

RESEARCH ARTICLE

10.1002/2014GC005232

Special Section:

Geodynamics of oceanic islands at slow-moving plates

Key Points:

- A 17.0 Ma record of Canary Island landslides exists in the Madeira Abyssal Plain
- This landslide record provides information on island provenance, age and volume
- There is no statistical correlation between landslide occurrence and climate

Supporting Information:

- Auxiliary material
- Figures S1, S2, S4–S6
- Tables S3, S7–S9

Correspondence to:

J. E. Hunt,
james.hunt@noc.ac.uk

Citation:

Hunt, J. E., P. J. Talling, M. A. Clare, I. Jarvis, and R. B. Wynn (2014), Long-term (17 Ma) turbidite record of the timing and frequency of large flank collapses of the Canary Islands, *Geochem. Geophys. Geosyst.*, *15*, 3322–3345, doi:10.1002/2014GC005232.

Received 8 JAN 2014

Accepted 10 JUL 2014

Accepted article online 14 JUL 2014

Published online 20 AUG 2014

Long-term (17 Ma) turbidite record of the timing and frequency of large flank collapses of the Canary Islands

J. E. Hunt[1], P. J. Talling[1], M. A. Clare[1], I. Jarvis[2], and R. B. Wynn[1]

[1]National Oceanography Centre, University of Southampton, Southampton, Hampshire, UK, [2]School of Geography, Geology and the Environment, Centre for Earth and Environmental Science Research, Kingston University London, Kingston upon Thames, Surrey, UK

Abstract Volcaniclastic turbidites on the Madeira Abyssal Plain provide a record of large-volume volcanic island flank collapses from the Canary Islands. This long-term record spans 17 Ma, and comprises 125 volcaniclastic beds. Determining the timing, provenance and volumes of these turbidites provides key information about the occurrence of mass wasting from the Canary Islands, especially the western islands of Tenerife, La Palma and El Hierro. These turbidite records demonstrate that landslides often coincide with protracted periods of volcanic edifice growth, suggesting that loading of the volcanic edifices may be a key preconditioning factor for landslide triggers. Furthermore, the last large-volume failures from Tenerife coincide with explosive volcanism at the end of eruptive cycles. Many large-volume Canary Island landslides also occurred during periods of warmer and wetter climates associated with sea-level rise and subsequent highstand. However, these turbidites are not serially dependent and any association with climate or sea level change is not statistically significant.

1. Introduction

The often exceptionally large scale of volcanic island submarine landslides was initially revealed by seafloor mapping, including evidence from the Hawaiian [*Moore et al.*, 1989, 1994; *McMurtry et al.*, 2004], Canarian [*Watts and Masson*, 1995, 2001; *Masson et al.*, 2002; *Acosta et al.*, 2003], Mascarene [*Oehler et al.*, 2004, 2008], Cape Verdean [*Le Bas et al.*, 2007; *Masson et al.*, 2008], Lesser Antilles [*Deplus et al.*, 2001; *Lebas et al.*, 2011; *Watt et al.*, 2012] and French Polynesian archipelagos [*Clouard et al.*, 2001; *Hildenbrand et al.*, 2006]. Volcanic island landslides can be far larger than any landslides on land. They can contain >200 km^3 of material, which compares to ~3.0 km^3 involved in the 1980 Mt St Helens landslide-eruption [*Voight et al.*, 1981]. Volcanic island landslides can potentially generate destructive tsunamis when they enter the surrounding ocean [*Kulikov et al.*, 1996; *Tinti et al.*, 1999, 2000; *Tappin et al.*, 2001; *Ward and Day*, 2003; *Fritz et al.*, 2009; *Giachetti et al.*, 2011]. Consequently, significant attention has been given to understanding volcanic island flank collapses and the hazards they may pose.

Volcanic islands commonly comprise rapidly constructed, steep flanks composed of interbedded pyroclastic deposits, lavas, and intrusive dykes [*McGuire*, 1996]. The presence of potentially weak strata and the injection of magmatic intrusions may be key factors affecting volcanic island flank stability [*McGuire*, 1996; *Elsworth and Day*, 1999; *Hürlimann et al.*, 1999a, 2000; *Masson et al.*, 2006; *Andrade and van Wyk de Vries*, 2010]. Preconditioning factors may include: (1) high sedimentation rates; (2) water saturation due to rising sea level; (3) elevated pore-fluid pressures; (4) high rainfall; (5) hydrothermal alteration; (6) deep narrow canyons reducing lateral strength; (7) faulting; (8) dyke intrusion; (9) seismic activity; (10) volcanic spreading; and (11) residual soils [*Siebert* 1984; *Siebert et al.*, 1987; *McGuire et al.*, 1990; *Elsworth and Voight*, 1995, 1996, 2001; *Murray and Voight*, 1996; *Day*, 1996; *McGuire*, 1996; *Voight and Elsworth*, 1997; *Hürlimann et al.*, 1999a, 2000, 2004; Masson *et al.*, 2006]. Recent studies have suggested a relationship between increased erosion and runoff, associated with the onset of warmer interglacial intervals, as a potentially important preconditioning factor [*McGuire*, 1992, 2010; *Keating and McGuire*, 2004; *McMurtry et al.*, 2004; *Deeming et al.*, 2010; *Tappin*, 2010; *Hunt et al.*, 2013a]. However, there are few field data sets suitable for testing rigorously these competing models for preconditioning factors and triggers. We are yet to monitor a major collapse in action and their causes remain poorly constrained.

One approach is to date major collapse events and to compare their timing to that of potential preconditioning factors and triggers. Onshore studies of volcanic island landslides rely on dating of the unconformities left behind by the mass movement. These dates often have significant uncertainties, since terrestrial records may include lengthy hiatuses and dating techniques may be limited. However, onshore volcanic island flank collapses have been shown to generate large submarine debris avalanches [*Moore et al*., 1989, 1994; *Watts and Masson*, 1995, 1998; *Ablay and Hürlimann*, 2000; *Deplus et al*., 2001; *Masson et al*., 2002, 2008; *Oehler et al*., 2004; *Le Bas et al*., 2007]. In turn, these debris avalanches may disaggregate and generate debris flows and turbidity currents that run out onto adjacent deep-water abyssal plains [*Garcia and Hull*, 1994; *Watts and Masson*, 1995; *Garcia*, 1996; *Masson*, 1996; *Wynn and Masson*, 2003; *Hunt et al*., 2011, 2013a, 2013b).

The near-continual deposition of pelagite sediments into which turbidites are interleaved provide a dateable record, whereby turbidite age is constrained by the ages of the underlying and overlying pelagites. This dateable pelagic record also has greater preservation potential since turbidity currents may be weakly or nonerosive at distances of >200 km from source [*Weaver and Kuijpers*, 1983; *Weaver and Thomson*, 1993; *Weaver*, 1994]. Therefore distal turbidite records allow relatively precise dating of the associated volcanic island landslides.

Here we present an analysis of an unusually long-term record of volcanic landslide-turbidites in the Madeira Abyssal Plain from ODP Sites 950, 951 and 952. These cores contain 125 volcaniclastic turbidites emplaced during an interval of 17 Ma. This large number of events enables robust statistical analysis, and helps to establish the most likely preconditioning factors of the collapses. The volcaniclastic turbidites of the Madeira Abyssal Plain have previously been inferred to have a Canary Island provenance [*Pearce and Jarvis*, 1992, 1995; *Jarvis et al*., 1998; *Hunt et al*., 2013a], and this study aims to further constrain their origin.

This is arguably the longest time series of major collapse events in any volcanic archipelago worldwide. Previous studies of Canary Island landslide-derived turbidites have only been able to resolve events in the last 1.5 Ma [*Weaver et al*., 1992; *Wynn et al*., 2002; *Hunt et al*., 2011, 2013a, 2013b). The longer time series of events can be used to better elucidate volcanic island landslide magnitude, frequency, and temporal clustering in the Canary Islands. These form crucial inputs for forward-looking geohazard assessments. Comparisons of landslide timing to climate change and volcanism provide a better understanding of preconditioning and trigger factors.

2. Aims

The aims of this article are set out as a series of questions:

1. How can distal mud-rich volcaniclastic turbidites provide information on the timing, provenance and magnitude of landslides?

2. How often does large-scale (>5 km^3) flank collapse occur in the Canary Islands?

3. Do flank collapses occur randomly or are they clustered in time?

4. Is there an association between the timing of flank collapses and volcanic activity?

5. Is there an association between the timing of flank collapses and sea level change, and hence climate?

3. Geological Setting

The Canary Islands comprise seven volcanic islands spread across ~500 km on the northwest African passive margin. They have developed in response to slow-movement of Jurassic-age (156–176 Ma) oceanic crust over a mantle plume [*Klitgort and Schouten*, 1986; *Anguita and Hernán*, 1990; *Hoernle and Schmincke* 1993; *Carracedo et al*., 1998; *Hoernle*, 1998]. This results in a general east-to-west age progression of the islands [*Carracedo*, 1994, 1999; *Carracedo et al*., 1998]. Recent landslide activity is most evident around the western Canary Islands of Tenerife, La Palma, and El Hierro, where Late Quaternary landslide activity has formed spatially extensive submarine debris avalanche deposits [*Masson et al*., 2002]. However, there is also evidence of past landslide activity from the older eastern Canary Islands [*Acosta et al*., 2003].

The focus of this study is the volcaniclastic turbidite history recorded in ODP cores from Sites 950, 951, and 952 in the Madeira Abyssal Plain (Figure 1). The Madeira Abyssal Plain represents the most distal and deepest depocentre in the Moroccan Turbidite System is located ~500 km west of the Canary Islands (Figure 1) [*Weaver and Kuijpers*, 1983; *Weaver et al*., 1992; Wynn *et al*., 2000, 2002]. The Madeira Distributary Channel

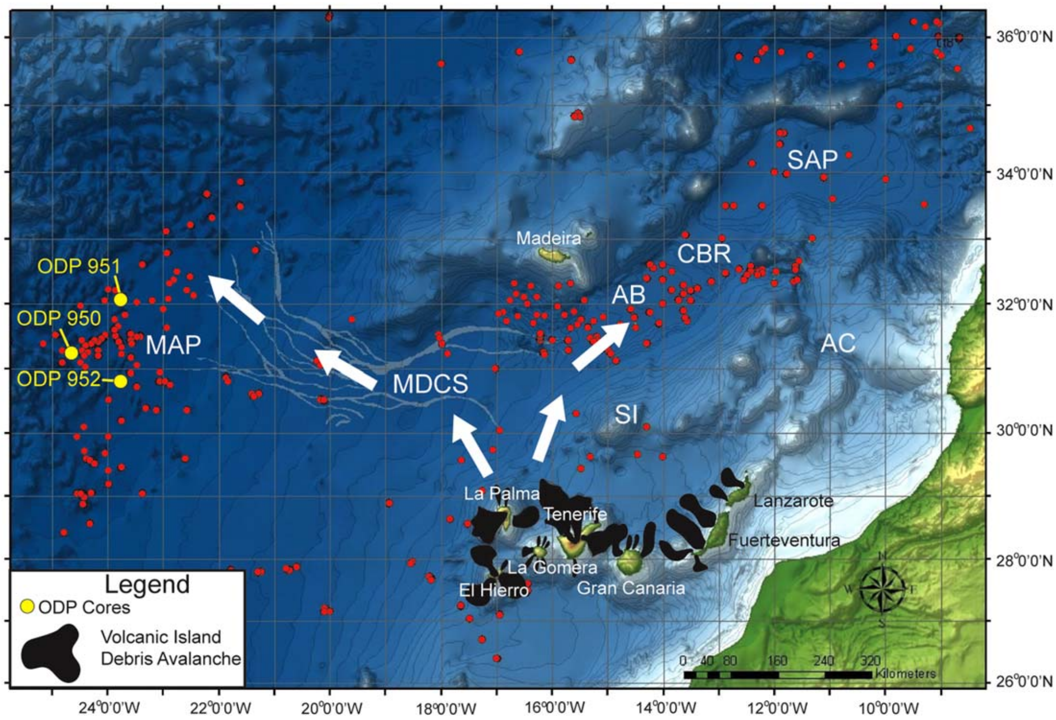

Figure 1. Map of the Moroccan Turbidite System, offshore Northwest Africa, showing the Madeira Abyssal Plain study area (MAP), Madeira Distributary Channel System (MDCS), Agadir Basin (AB), Seine Abyssal Plain (SAP), Selvagen Islands (SI), Agadir Canyon (AC) and Casablanca Ridge (CBR). Map illustrates the position of the ODP Sites utilized in this study and the turbidity current pathways. White arrows indicate the pathways of volcanic island-sourced turbidity currents [*Pearce and Jarvis*, 1992; *Frenz et al*., 2009]. Red circles indicate locations of shallow piston cores.

System connects the Madeira Abyssal Plain to the Canary Islands and Agadir Basin [*Masson*, 1994; *Stevenson et al*., 2013].

The turbidites represent landslides from Canary Islands. Their magnitude is greater than river discharges at >1 km^3, and commonly >20 km^3. These turbidites are also unlikely to be pyroclastic flows that have entered the sea and become turbidity currents. The largest volumes of pyroclastic material proximally onshore are of an order less than 20 km^3 on Tenerife [*Edgar et al*., 2007], thus the runout distance of >1000 km and volume of the turbidites in the basin being 20–380 km^3 support these being landslide derived. Small-scale submarine landslides from both Madeira and the Selvagen Islands have been identified [*Frenz et al*., 2009; *Hunt et al*., 2013c], however mapping of Quaternary deposits suggest these are restricted to the local slopes of these sources and so not enter the Madeira Channels and travel to the Madeira Abyssal Plain [*Stevenson et al*., 2013; *Hunt et al*., 2013c].

4. History of Landslides Within the Canary Islands

Numerous studies have documented the volcanic and geomorphological evolution of the Canary Islands. This section aims to summarize the onshore and proximal marine records of landslides in the Canary Islands, which then will then be compared to the distal turbidite record.

4.1. Fuerteventura and Lanzarote

Stillman [1999] documented the mass-wasting phases of Fuerteventura. Numerous onshore landslides have been dated between 22 and 16.5 Ma, and could be linked to old collapses of the Central and Southern Volcanic Complexes (>17.5 Ma; Table 1) [*Acosta et al*., 2003]. There is little literature documenting flank collapses from Lanzarote (Table 1). Large denuded and scalloped coastlines northwest of the Famara volcanic complex and southeast of the Los Ajaches volcanic complex may indicate large-scale flank collapses. However, neither Lanzarote nor Fuerteventura has evidence of major landslide activity that postdates 15 Ma.

Table 1. Summary of Volcanic Flank Collapses From Fuerteventura, Lanzorote,Gran Canaria and La Gomera in the Canary Islands[a]

Event	Type	Age	Volume (km^3)	Area (km^2)	Comments
Fuerteventura					
Central Volcanic Complex I Collapse	Slide	~22 Ma[b,c]	?	?	Deduced from an unconformity between Central Volcanic Complex (CVC) lavas II and I. Fractured nature of CVC I and steeper dip infers landslide event.[c]
Central Volcanic Complex II Collapse (Puerto Rosario)	Slide and DA	20-16.5 Ma[c]	?	3500[d]	Unconformity below Melindraga and Tamacite formations.[c] Offshore evidence of buried event.[d]
Southern Volcanic Complex Collapse (Southern Puerto Rosario)	Slide and DA	>17.5 Ma[c]	?	1200[d]	Offshore evidence of buried debris avalanche cut by gullies on opposing slope of scalloped southern shoreline.[d]
Unknown	DF	17.6 Ma[e]	?	?	Volcaniclastic debris flow v4 from DSDP Site 397.[e]
Unknown	DF	17.2 Ma[e]	?	?	Volcaniclastic debris flow v3 from DSDP Site 397.[e]
Unknown	DF	17.0 Ma[e]	?	?	Volcaniclastic debris flow v2 from DSDP Site 397.[e]
Unknown	DF	16.5 Ma[e]	?	?	Volcaniclastic debris flow v1 from DSDP Site 397.[e]
Jandía	DA	~2 Ma[f]	25[g]	250[g]	Identified in sidescan sonar.[g] Also mapped in swath bathymetry.[d]
Eastern Canary Ridge	DF	<100 ka[g]	>20[g]	>2000[g]	Mapped using swath bathymetry, sidescan sonar and shallow 3.5kHz seismic reflections.[g]
Lanzarote					
Unknown	Slide	18-16 Ma[d]	?′	>800[d]	Buried event poorly constrained[d], possibly collapses of Los Ajaches and Famara complexes.
Gran Canaria					
Agaete (Caldera de Tejeda)	Slump and DA	~14 Ma[d,h]	>50[g]	200–500[d,g]	Erosional collapse of early basaltic shield.[h] Scalloped north-west shoreline and offshore bathymetry.[d] Two potential debris avalanches in apron ODP Site 953.[i] Also identified in seismic reflection.[j]
Horgazales Basin	DA	14–15 Ma[g]	>80[g]	>1000[g]	Identified in seismic reflection profiles and from ODP leg 157.[i,j]
Pre-Galdar	DA	12–15 Ma[g]	>60[g]	>700[g]	Identified in seismic reflection profiles and ODP leg 157.[i,j]
Fataga Collapses	DFs	9–11.5 Ma[k]	?	?	Series of trachyphonolite-rich debris flow units encountered in ODP hole 953, related to collapses of the Fataga volcano.[k]
Las Palmas	DA	9 Ma[d]	?	1100[d]	Older event on the northeast flank of Gran Canaria.[d]
Roque Nublo	DA	3.9-3.5[d]	~34[g]	150–330[d,g]	Forms over the area of the Las Palmas debris avalanche lobe.[d] However, debris avalanche on southwest flank identified as Roque Nublo event.[f,l]
Galdar	DA	3.9-3.5[d]	?	300[d]	Forms a lobe on the northern flank of Gran Canaria.[d]
La Gomera					
Unknown	DFs	~12 Ma[m]	?	?	Four highly primitive basalt-rich debris flow deposits encountered at ODP hole 956, linked to early basaltic shield development on La Gomera.[m]
Tazo	DA	9.4–8.6[n]	?	?	Northwest-directed 150 m-thick breccia onshore.[n]
San Marcos	DA	9.4–8.6[n]	?	?	Onshore breccias below Tazo deposit.[n]
I	DF	~4.0 Ma[d]	?	80[d]	Mapped using swath bathymetry.[d]
II	DF	~4.0 Ma[d]	?	80[d]	Mapped using swath bathymetry.[d]
III	DF	~4.0 Ma[d]	?	340[d]	Mapped using swath bathymetry.[d]
IV	DF	~4.0 Ma[d]	?	160[d]	Mapped using swath bathymetry.[d]
V	DF	~4.0 Ma[d]	?	300[d]	Mapped using swath bathymetry.[d]
VI	DF	~4.0 Ma[d]	?	40[d]	Mapped using swath bathymetry.[d]
VII	DF	~4.0 Ma[d]	?	50[d]	Mapped using swath bathymetry.[d]
VIII	DF	~4.0 Ma[d]	?	300[d]	Mapped using swath bathymetry.[d]

[a]DA = debris avalanche, DF = debris flow
[b]*Ancochea et al.* [1996].
[c]*Stillman* [1999].
[d]*Acosta et al.* [2003].
[e]*Schmincke and von Rad* [1979].
[f]*García and Cacho* [1994].
[g]*Krastel et al.* [2001].
[h]*Van den Bogaard and Schmincke* [1998].
[i]*Schmincke and Segschneider* [1998].
[j]*Funck and Schmincke* [1998].
[k]*Schmincke et al.* [1995].
[l]*Mehl and Schmincke* [1999].
[m]*Schmincke and Sumita* [1998].
[n]*Ancochea et al.* [2006].

4.2. Gran Canaria

The first major phase of erosion occurred at ~14.0 Ma with collapse and formation of the Caldera de Tejeda [*van den Bogaard and Schmincke*, 1998], producing the Agaete debris avalanche (Table 1). ODP core from the northern and southern aprons of Gran Canaria (Sites 953–956) show a long history of small-volume (<5 km^3) volcaniclastic turbidites between 4.5 and 3.5 Ma, coinciding with onshore debris avalanches [*García Cacho et al*., 1994; *Carey et al*., 1998; *Goldstrand*, 1998; *Schmincke and Segschneider*, 1998; *Mehl and Schmincke*, 1999; *Acosta et al*., 2003]. No large-volume island flank landslides have been identified after 3.5 Ma (Table 1) [*Acosta et al*., 2003].

4.3. La Gomera

Acosta et al. [2003] identified eight debris avalanche lobes from swath bathymetry of the submarine flanks (Table 1). Three lobes occur on the northern flank, one to the east, two on the southern flank and two to the west. *Llanes et al*. [2009] further interpreted a series of scalloped embayments on the northern margin and numerous flat-bottomed canyons on the southern margin as a series of headwall scarps.

4.4. Tenerife

It has been proposed that several landslides were initiated from the Teno Massif between 6.3 and 6.0 Ma, and these were responsible for both the onshore unconformities above the Masca Formation and an offshore debris avalanche (Table 2) [*Walter and Schmincke* 2002; *Masson et al*., 2002; *Acosta et al*., 2003; *Leonhardt and Soffel*, 2006; *Longpré et al*., 2009]. The Anaga Massif collapsed at 4.7-4.1 Ma (Table 2) [*Masson et al*., 2002; *Acosta et al*., 2003; *Llanes et al*., 2003; *Walter et al*., 2005]. The Tigaiga debris avalanche is another failure from the northern flank of Tenerife (Table 2), which has been tentatively dated at >2.3 Ma [*Cantagrel et al*., 1999; *Krastel et al*., 2001; *Acosta et al*., 2003].

On the southern flank of Tenerife a 25 km^3 failure between 2.0 and 0.7 Ma has been reported, termed the Bandas del Sur debris flow or Abona avalanche [*Krastel et al*., 2001; *Harris et al*., 2011]. The eastern flank of Tenerife is the site of the Güímar landslide, dated at 0.8-0.78 Ma (Table 2) [*Ancochea et al*., 1990; *Cantagrel et al*., 1999; *Krastel et al*., 2001; *Masson et al*., 2002]. A number of failures younger than 2.0 Ma have been reported on the northern flank of Tenerife, including the Roques de García, Orotava and Icod landslides (Table 2).

4.5. La Palma

The Cumbre Nueva structure represents a collapse dated at either 558 ka [*Acosta et al*., 2003] or 566-533 ka [*Carracedo et al*., 2001]. It overlies the Playa de la Veta deposit immediately offshore, and is highlighted by a higher backscatter sonar response compared to the older Playa de la Veta debris avalanche [*Urgeles et al*., 1999; *Masson et al*., 2002]. *Masson et al*. [2002] identified an additional flank collapse, which resulted in the Santa Cruz landslide from the eastern flank of La Palma. Landslide activity has also been identified on the northern flank, but this has not been dated or quantified [*Acosta et al*., 2003].

4.6. El Hierro

Tiñor lavas are found below an angular unconformity dated at 1.04 Ma within the El Golfo embayment, and may represent an older major landslide [*Carracedo et al*., 1999]. The El Julán landslide occurred on the southwest flank of El Hierro between 500 and 300 ka. The Las Playas I and II debris avalanche complex was defined by *Gee et al*. [2001] and *Masson et al*. [2002] on the southeast flank, with ages of 545-176 ka for Las Playas I and 176-145 ka for Las Playas II (Table 2). The El Golfo landslide represents the youngest volcanic flank collapse in the Canary archipelago [*Weaver et al*., 1992; *Wynn et al*., 2002; *Wynn and Masson*, 2003; *Frenz et al*., 2009]. The likely date is 15 ka, which is based on a midpoint of onshore ages and from study of the associated turbidite deposit (Table 2) [*Masson*, 1996].

5. Previous Work on the Madeira Abyssal Plain Turbidites

The stratigraphy and provenance of Madeira Abyssal Plain turbidites in the last 780 ka is well established [*Weaver et al*., 1992; *Wynn et al*., 2002; *Hunt et al*., 2013a]. The turbidites of this stratigraphy have a lettered nomenclature with the youngest starting at *A*, and with an "M" prefix that denotes the Madeira Abyssal Plain [*Wynn et al*., 2002; *Hunt et al*., 2013a]. The "M" prefix is dropped here for convenience.

Table 2. Summary of Volcanic Flank Collapses From Tenerife, La Palma, and El Hierro in the Canary Islands

Event	Type	Age	Volume (km^3)	Area (km^2)	Comments
Tenerife					
Masca (Los Gigantes)	DA	5.89-6.65 Ma[a,d]	?	?	The Masca unconformity marks the first major collapse recorded onshore in the Teno massif.[a] Numerous studies have attempted to date this event, with dates lying around ~6.4 Ma.[a,d]
Carrizales	DA	5.89-6.27 Ma[a,d]	?	?	The Carrizales marks a second major unconformity in the onshore Teno Massif.[a] Numerous studies have dated this, with an accepted date of ~6.1 Ma.[d]
Teno	DA	~6.0 Ma[c,g]	?	400[e]	Offshore debris avalanche mapped using swath bathymetry and sidescan sonar.[e,g] Could represent either Masca and/or Carrizales events, or a separate event altogether.
Anaga	DA	4.1–4.7 Ma[h]	36[i]	>400[g]	Mapped using swath bathymetry and sidescan sonar.[e,g]
Tigaiga	Slide and DA	2.3-2.6 Ma[c,g]	?	200[e]	Onshore deposit in addition to a buried deposit on the northern flank of Tenerife.[f,j]
Bandes del Sur	DA	<2 Ma[f]	25[f]	500[f]	Mapped off the southern flank of Tenerife using sidescan sonar.[f]
Roques de García	DA	0.6-1.3 Ma[c,k]	~500[c,g]	2200–4500[e,g]	Mapped using sidescan sonar, shallow 3.5 kHz seismic reflection, and swath bathymetry.[e,l] Dating of turbidite linked to event is 860±25 ka.[m,n]
Güímar	DA	830–850 ka[n,o]	44–120[g,o]	1600[g]	Mapped using swath bathymetry.[e]
Orotava	Slide and DA	505–530 ka[n,o]	500[g,k]	2100[g,k]	Debris avalanche deposit mapped using sidescan sonar and swath bathymetry.[e,q] Onshore dating range has been limited to 540–690 ka.[c,l] However, associated turbidite has been dated at 530±25 ka.[m]
Icod	Slide and DA/DF	165 ka[r]	320[r]	1,700[g,k]	Debris avalanche deposits mapped using sidescan sonar and swath bathymetry.[e,q] Onshore dating of the event is between 150 and 170 ka.[c,g] Dating of the debris avalanche from the sediment drape is ~170 ka.[l] The turbidite in Agadir Basin has been dated at 160–165.[r–t]
La Palma					
East Puerto del Mudo	DA	>1.0 Ma?[e]	?	400[e]	Mapped in swath bathymetry.[e]
West Puerto del Mudo	DA	>1.0 Ma?[e]	?	>300[e]	Mapped in swath bathymetry.[e]
Playa de la Veta	DA	1.185 Ma[g,u]	520–650[f,u]	1,200-2,000[f,u]	Mapped using sidescan sonar, shallow seismic reflection and swath bathymetry.[e,v]
Santa Cruz	DA	0.9-1.2 Ma[e,w]	?	1,600[e]	Mapped using swath bathymetry.[e]
Cumbre Nueva	DA	~520 ka[g,u]	80–95[g,u]	700–780[g,x]	Mapped using sidescan sonar, shallow seismic reflection and swath bathymetry.[e,v] Correlated turbidite in the Madeira Abyssal Plain dated at 485±25 ka[m]
El Hierro					
Tiñor	DA (buried)	0.54-1.12 Ma[w,y]	?	?	Theorized collapse from an unconformity in mining gallerias.[y] Correlated turbidite from Madeira Abyssal Plain dated at 1,050±25 ka.[m]
San Andréas	Aborted Slump	176–545 ka[z]	?	?	Studied from onshore faults.[z] Could be related to early phases of failure during Las Playas I or II events, certainly the dates coincide with those for Las Playas events.[g]
Las Playas I	DA	176–545 ka[g]	?	1,700[g,x]	Broader debris avalanche with smoother sediment cover, mapped with sidescan sonar.[g]
El Julan	DA	320–500 ka[A,B]	60–130[e,g]	1,600-1,800[f,B]	Mapped using sidescan sonar, seismic reflection profiles and swath bathymetry, but little onshore record.[e,g] Correlated turbidite from Madeira Abyssal Plain dated at 540±20 ka.[m]

10.1002/2014GC005232

Table 2. (continued)

Event	Type	Age	Volume (km^3)	Area (km^2)	Comments
Las Playas II	Failed slump with minor DA/DF	145–176[g,u]	~50[g,u]	950[g,x]	Confined elongate debris flow/avalanche.[g,u]
El Golfo	DA	15[n,u,A,C]	150–180[A]	1,500-1,700[e,A]	Mapped using sidescan sonar, swath bathymetry and shallow seismic reflection.[e,A] Correlation to a large-volume volcaniclastic turbidite in Agadir Basin and Madeira Abyssal Plain.[r,D]

[a]*Longpré et al.* [2009].
[b]*Leonhardt and Soffel* [2006].
[c]*Cantagrel et al.* [1999].
[d]*Walter and Schmincke* [2002].
[e]*Acosta et al.* [2003].
[f]*Krastel et al.* [2001].
[g]*Masson et al.* [2002].
[h]*Walter et al.* [2005].
[i]*Llanes et al.* [2003].
[j]*Marti and Gudmundsson* [2000].
[k]*Watts and Masson* [1998].
[l]*Watts and Masson* [1995].
[m]*Hunt et al.* [this study].
[n]*Hunt et al.* [2013a].
[o]*Giachetti et al.* [2011].
[p]*Ablay and Hürlimann* [2000].
[q]*Hürlimann et al.* [2004].
[r]*Wynn et al.* [2002].
[s]*Frenz et al.* [2009].
[t]*Hunt et al.* [2011].
[u]*Urgeles et al.* [1999].
[v]*Urgeles et al.* [2001].
[w]*Carracedo* [1999].
[x]*Urgeles et al.* [1997].
[y]*Carracedo et al.* [1999].
[z]*Day et al.* [1997].
[A]*Masson* [1996].
[B]*Holcomb and Searle* [1991].
[C]*Guillou et al.* [1995].
[D]*Weaver et al.* [1992].

The record includes volcaniclastic turbidites *B* (15 ka) and *G* (190-160 ka), representing the El Golfo and Icod landslides from the Western Canary landslides respectively [*Wynn et al*., 2002; *Wynn and Masson*, 2003]. In addition, older volcaniclastic turbidites, beds *N*, *O* and *P* (540-485 ka) are interpreted to represent the Cumbre Nueva, Orotava, and El Julan landslides from La Palma, Tenerife, and El Hierro respectively [*Weaver et al*., 1992; *Hunt et al*., 2013a]. Interrogation of the 1.5 Ma to recent record identified three further turbidites *Z*, *AB*, and *AF* dated between 1.2 and 0.8 Ma. These deposits most likely represent the Güímar, El Tiñor, and Roque de García landslides, respectively [*Hunt et al*., 2013a]. Furthermore, information gleaned from these eight turbidites indicates that the associated landslides were multistage [*Hunt et al*., 2013b].

5.1. Methodology and Data

Cores from ODP Sites 950, 951, and 952 were used in this study. The first objective was to resolve the ages of individual volcaniclastic turbidites in the 17-0 Ma sediment record, using the biostratigraphy and magnetostratigraphy of *Howe and Sblendorio-Levy* [1998]. Previous work has reported the frequency of volcanic island landslides as the number of events were million years. This work focuses on these individual events. Second, the geochemistry of these volcaniclastic turbidites were investigated using the results previously published by *Jarvis et al*. [1998], together with new unpublished trace element geochemical data. Third, the volumes of these deposits were calculated using the methodology of *Weaver* [2003], based on a methodology from *Van Hinte* [1978] with volumes from *Rothwell et al*. [1998]. Lastly, the landslide record derived from the Madeira Abyssal Plain ODP cores was compared to the documented onshore Canary Island landslide histories.

5.2. ODP Stratigraphy

The 17 to 0 Ma stratigraphy of the Madeira Abyssal Plain has been constructed using three sites (950, 951 and 952) from ODP Leg 157 (Figure 1). Turbidites were correlated between the three sites using their position in the vertical sequence, colour, magnetic susceptibility, and biostratigraphy. The biostratigraphy and magnetostratigraphy of *Howe and Sblendorio-Levy* [1998] was used to provide dated horizons that allow pelagite ages to be extrapolated between datum levels. The turbidite chronology is calculated from its position within the dated pelagite sequence. Turbidite chronology is independently derived for each ODP site based on pelagic sedimentation rates (Figure 2 and supporting information Appendices 1 and 2). Dating of singular turbidites utilizing hemipelagite coccolithosphore biostratigraphy and hemipelagite photospectral composition have yielded potential dating errors of ±10 ka for those beds younger than 1.5 Ma [*Hunt et al*., 2013a]. Robust coccolithophore biostratigraphy extends to 7.0 Ma. Thus landslides dated from 7.0 Ma to recent may have conservative dating errors of ±10 ka. Dates for events older than 7.0 Ma may have greater errors due to the greater paucity of biostratigraphic datum horizons and potential for variable sedimentation rates.

5.3. ODP Turbidite Geochemistry

Bulk geochemical analyses were undertaken and presented by *Jarvis et al*. [1998], using 10 mL samples taken from the mudcaps of turbidites >20 cm thick at Site 950. The preparation and methodology is described in *Jarvis et al*. [1998]. Additional trace element data for these samples is also presented. These additional trace element data were obtained by ICP-MS analysis of lithium metaborate fusion and HF-perchloric acid digest solutions, following the methods of *Totland and Jarvis* [1997] and *Jarvis* [2003]. For comparison of mudcap compositions between turbidites, samples from a single bed are averaged.

5.4. Turbidite Volumes Based on ODP Studies

Turbidite volumes have been calculated according to the method of *Weaver* [2003]. Turbidite volumes are reported as the decompacted volume upon deposition, which effectively provides the volume of the sediment carried by the flow. This allows better comparisons of event magnitude between younger and older events. Here the turbidite volumes were generated based on the ratio of turbidite decompacted thickness to the decompacted thickness of the seismic unit in which it resides. This was then compared against the calculated decompacted volume of the respective seismic unit [*Alibés et al*., 1996, 1999]. The methodology is described in more detail in supporting information Appendices 3 and 4.

6. Results

6.1. Turbidite Characterization

It is essential to isolate the volcaniclastic turbidites from the mixed siliciclastic-volcaniclastic record. The Late Quaternary sequence of the Madeira Abyssal Plain contains turbidites of three broad types: organic-rich siliciclastic (>0.3% TOC), volcaniclastic (>0.6 Ti/Al) and calcareous (low Ti/Al and >78% $CaCO_3$) [*De Lange et al*., 1987; *Pearce and Jarvis*, 1992, 1995]. There are also brown beds from local seamount collapses and metre-thick pale gray "nonvolcanic" beds that most likely originated from the submarine regions around the Canary Islands [*Jarvis et al*., 1998; *Lebreiro et al*., 1998; *Weaver et al*., 1998]. These deposits can be characterized by the mudcap geochemistry using a series of cross plots (Figure 3) and using the ternary plots of *De Lange et al*. [1987] (supporting information Appendix 5).

The organic-rich green siliciclastic turbidites generally have compositions separate from the volcaniclastic turbidites, and from the white calcareous and pale gray "nonvolcanic" beds. The pale gray "nonvolcanic" beds show similarities between the volcaniclastic and calcareous turbidites but are compositionally different from either. The gray volcaniclastic turbidites that are the focus of this study are both geochemically distinct and have greater magnetic susceptibility.

The volcaniclastic turbidites have generally <3.5 wt% MgO and <3.5 wt% K_2O carbonate-free-basis (CFB) compositions, while for higher concentrations of TiO_2 the sediments are Al-poor (i.e., exhibit high Ti/Al ratios) (Figure 3). Lastly, they are generally characterized by having >200 ppm Zr and carbonate contents of >30 wt% (Figure 3).

6.2. Volcaniclastic Turbidite Composition Through Time

The ODP turbidite record forms two parts: a pre-7.0 Ma and post-7.0 Ma component. Apart from a few thin (10–50 cm) turbidites, the post-7.0 Ma stratigraphy can be correlated between the upper 230 m of the three ODP Sites (Figures 4–7). These correlations are supported by biostratigraphy (Figure 2), lithostratigraphy

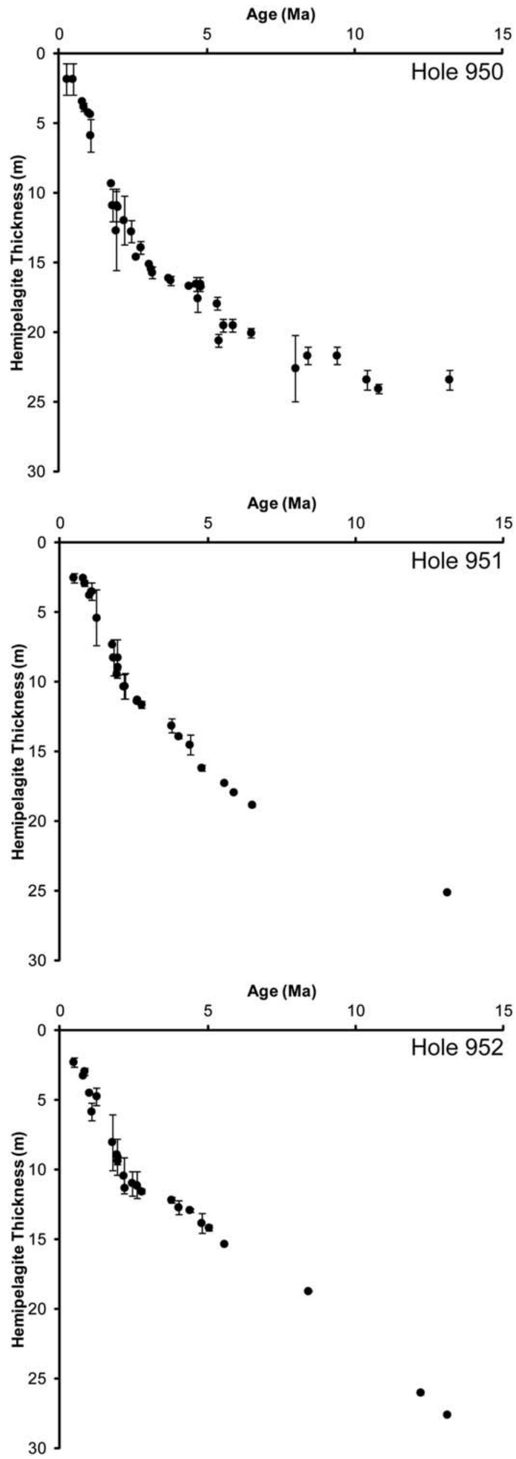

Figure 2. Pelagite age profiles for ODP Sites 950, 951, and 952. Dates based on coccolith biostratigraphy and magnetostratigraphy presented in *Howe and Sblendorio-Levy* [1998]. Error bars represent the thickness of pelagic sediment over which the age was derived.

and magnetic susceptibility profiles (Figures 4–7). The correlations are characterized in a series of correlation panels depicting the Pleistocene (Figure 4), Upper Pliocene (Figure 5), Lower Pliocene (Figure 6) and uppermost Miocene (Figure 7). The turbidites in general are typically 0.5 to 11.0 m-thick, while the volcaniclastic turbidites range from 0.5 to 4.0 m in thickness.

The post-7.0 Ma volcaniclastic turbidites have decompacted volumes between 5 and 380 km^3, which far exceed the thickness and decompacted volumes present in the pre-7.0 Ma history (Figure 8). There is a distinct shift in the dominant composition in the post-7.0 Ma volcaniclastic turbidites (Figure 9), which includes beds with significantly higher Ti, Zr, K, and Mg contents.

The Zr/Al-Ti/Al cross plot shows three compositional groups of increasing Zr/Al and Ti/Al (Figure 10a). There are three groups derived from K/Al-Cr/Al cross plots showing increasing K/Al with generally decreasing Cr/Al (Figure 10b), and three groups from Si/Al-Mg/Al showing increasing Si/Al with decreasing Mg/Al (Figure 10c). The pre-7.0 Ma volcaniclastic record is characterized by 0.2 to 1.0 m thick gray and dark-gray volcaniclastic turbidites, which cannot be correlated between Sites 950, 951, and 952 with any certainty. The volumes of these pre-7.0 Ma volcaniclastic turbidites are relatively small, with most being <10 km^3 (Figure 8). The turbidites are also characterized by relatively low Ti, Zr, K and Mg, with relatively higher Si and Cr contents (Figures 9 and 10). Trace element and rare-earth element (REE) trends also show distinctive compositional characters. Indeed, those turbidites with basaltic and primitive compositions have signatures generally reflecting high TiO_2-$MgO+Fe_2O_3$, TiO_2-Ni, La/Th-Hf, Zr/Sc and Th/Sc (supporting information Appendix 6).

6.3. Source and Timing of Volcaniclastic Turbidites

This section uses the calculated ages of the volcaniclastic turbidites coupled with information from the mudcap geochemistry to identify the potential source island of the landslide.

6.3.1. Mid-Late Miocene 7.0–6.0 Ma Record

The first metre-thick volcaniclastic turbidites occur after 7.0 Ma, with an initial sequence of beds *FT* to *FD* from 7.0 to 6.0 Ma (Figure 7). These volcaniclastic beds represent the thickest and most voluminous turbidites of this period, and bed *FK* is the largest volcaniclastic bed recorded in the Madeira Abyssal Plain (4 m thick and 380 km^3-volume) (Figure 7).

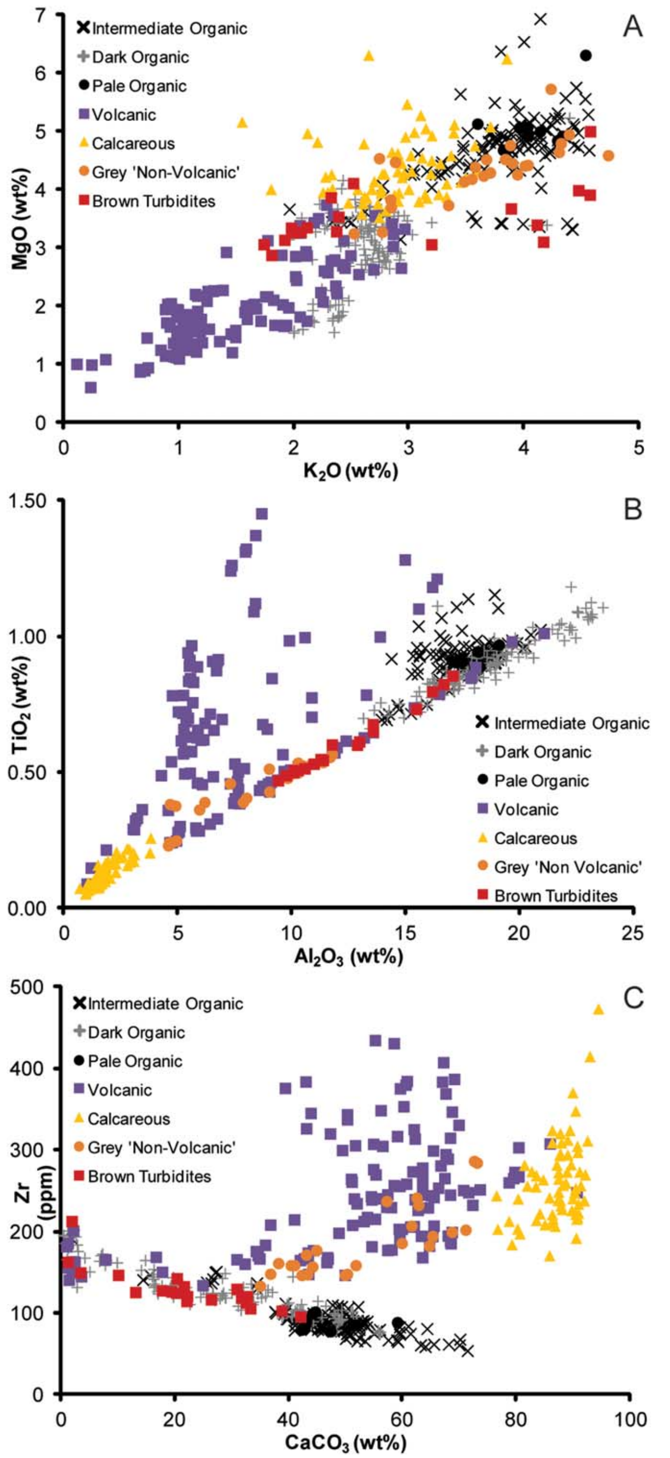

Figure 3. Bulk geochemical cross plots of mudcap compositions for all turbidites in the Madeira Abyssal Plain. Elements plotted on a carbon-free basis. Highlights the different compositions of organic-rich siliciclastic (dark, intermediate and pale green), volcaniclastic, calcareous, pale gray "nonvolcanic" and brown turbidites.

Bed *FT* has moderate Zr, Ti, and Mg, high K and low Si, signifying a basic, but not depleted composition (Figure 10). Beds *FS* and *FR* have low Zr, Ti, and Si, moderate Cr and high K, indicating more basic compositions, but are relatively low in volume. Beds *FP*, *FO*, *FM*, *FL* and *FD* have high-to-moderate Ti, high Zr and K, and low-to-moderate Mg and Si, which signify evolved compositions similar to those of younger turbidites *G*, *O* and *Z* from Tenerife (Figure 10). Excluding bed *FK*, there is a trend from beds *FT* to *FD* toward an increasingly evolved composition. The aforementioned bed *FK* has a basic composition.

6.3.2. Early Pliocene 5.3–4.0 Ma Record

The thickest and largest volume turbidites in this sequence are beds *EK* and *DK*, representing 1.5–2.0 m thick and 50–60 km^3 deposits (Figure 6). These beds have evolved compositions, with bed *DK* at 4.2 Ma having a similar composition to turbidites of Tenerife provenance (Figure 10). The other turbidites (beds *EI*, *EH*, *DZ*, *DY*, *DU*, *DL* and *DF*) are basic to trace-element depleted in composition, but with increased K (Figure 10).

6.3.3. Late-Early Pliocene 3.7-3.0 Ma Record

This time period commenced with a 1.75 m thick turbidite at 3.75 Ma (bed *DB*) (Figure 6). Turbidite *DB* has low Zr and Ti, but high K and Mg (Figure 10), thus having properties similar to turbidites from the pre-7.0 Ma record associated with a basic and trace element-depleted origin [*Jarvis et al.*, 1998]. However, bed *DB* also has an evolved REE composition, i.e., a high La/Sc ratio (supporting information Appendix 9). The following turbidites (beds *CV1*, *CT2* and *CT4*) are thin-bedded and low-volume events with basic compositions. Bed *CS* (3.25 Ma) represents the thickest and most volumetric event in this time interval (2–4 m thick and 110 km^3). This event has a basic composition of high Ti and Mg, and moderate Si, K, Cr,

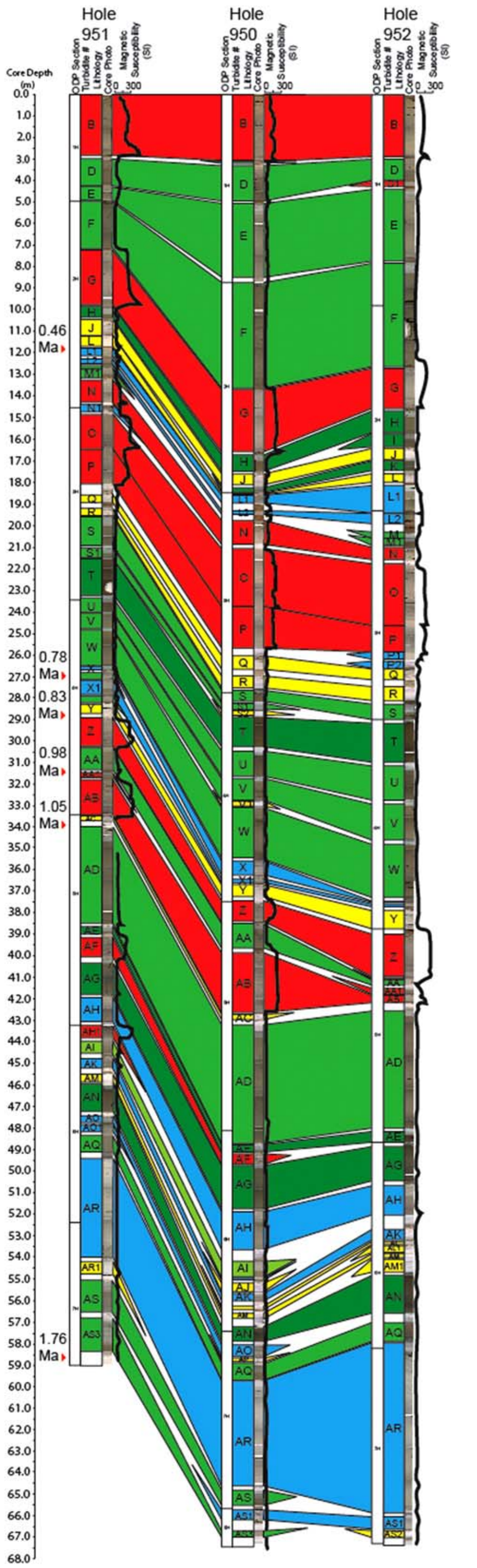

Figure 4. Correlation panel of ODP holes 950, 951, and 952 showing Pleistocene-age turbidites in the Madeira Abyssal Plain. Ages from *Howe and Sblendorio-Levy* [1998].

and Zr, similar to those ascribed to El Hierro (Figure 10), however it has an evolved trace-element and REE composition (supporting information Appendix 9), and El Hierro was not present at this time. The last deposits of this time interval (beds *CR* and *CM*) are similar to bed *DB* (Figure 10), but both have primitive basaltic REE compositions (Figure 12).

6.3.4. Late Pliocene 2.6-1.8 Ma Record

This turbidite sequence includes thin-bedded turbidites (<0.5 m thick) and metre-thick voluminous turbidites (1–4 m thick), including beds *BZ*, *BQ*, *BN*, *BF*, *BC*, *BB*, *AV*, *AU*, and *AT*. Bed *BF*, dated at ∼2.2 Ma, represents the thickest and largest volume deposit in this time interval, and it has a composition of high Zr, K, Mg, and Cr and low Ti (Figure 10), with a similar composition to those previously assigned to a Tenerife provenance. Beds *BZ*, *BQ*, and *AT* have low Zr and Ti, but moderate-to-high K and Mg. Beds *BN*, *BC*, *AV*, and *AU* have moderate (basic) Zr and Ti, and moderate-to-high K and Mg, similar to those ascribed to a La Palma or El Hierro provenance (Figure 10).

6.3.5. Pleistocene 1.5-0 Ma Record

This record has been studied previously and was briefly reinvestigated in the present study [*Pearce and Jarvis*, 1992, 1995; *Weaver et al.*, 1992; *Hunt et al.*, 2013a]. The record represents a number of turbidites of evolved and basic compositions that can be correlated to Tenerife and western Canary Island provenances. The compositions have high Zr, K, and Mg and high to moderate Ti and Si (Figure 10). These turbidites can be grouped into two compositional groups: a basic igneous group (Group 1) defined by low Zr and K_2O, and high TiO_2, MgO, and Fe_2O_3, and an evolved igneous group (Group 2) with higher Zr and K_2O, but lower TiO_2, MgO and Fe_2O_3 [*De Lange et al.*, 1987; *Pearce and Jarvis*, 1992, 1995].

Group 1 includes beds *B* (0.015Ma), *P* (0.54 Ma), and *AB* (1.05 Ma). Group 2 includes beds *G* (0.165 Ma), *O* (0.535 Ma), and *Z* (0.84 Ma) [*Hunt et al.*, 2013a; Figure 10). However, beds *N* and *AF* have less distinct compositions, displaying geochemical affinities for both Groups 1 and 2. Bed *AF* represents the oldest deposit in this period at ∼1.2 Ma, and likely originated from Tenerife based on its evolved composition and an affiliation with Group 2 beds of Tenerife provenance. Bed *N*, at ∼0.49 Ma has a composition showing disparities with both Groups 1 and 2. Trace-element and REE data display other differences between the groups, where Group 1 has higher Th/Sc, Zr/Sc and La/Sc compared to Group 2. Bed *N* shows an affinity for Group 2, whilst bed *AF* lacks REE data to interpret.

10.1002/2014GC005232

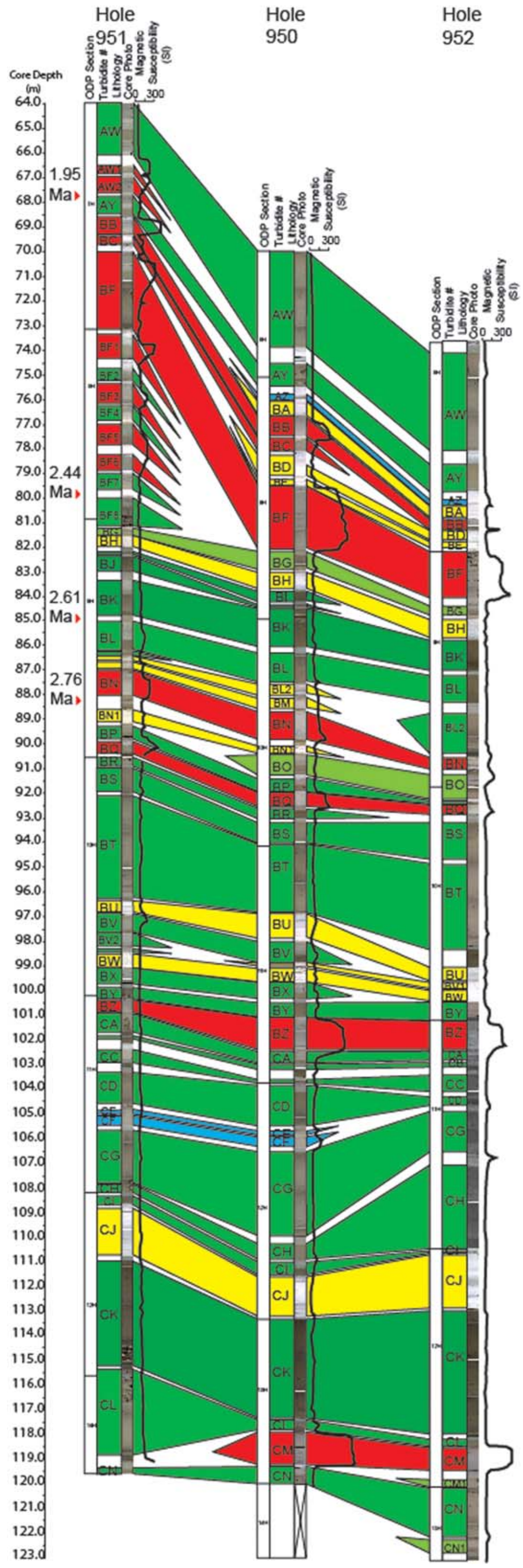

Figure 5. Correlation plot of ODP holes 950, 951, and 952 showing Late Pliocene-age turbidites in the Madeira Abyssal Plain. Dates from *Howe and Sblendorio-Levy* [1998]. Turbidite legend from Figure 4.

6.4. Statistical Analyses of Landslide Recurrence

The volcaniclastic turbidite record has been separated into 17 Ma to 7 Ma and 7 Ma to recent periods. Between 17 Ma and 7.0 Ma there are variable records of volcaniclastic turbidites at the three ODP Madeira Abyssal Plain sites (Figure 11). Since 7 Ma there has been an increase in the thickness of the volcaniclastic turbidites, and thus the volume of the deposits, possibly as a result of changes to the turbidite pathway, as this change is also seen in siliciclastic turbidites [*Weaver et al.*, 1998]. These changes may represent structural changes to the continental rise that restrict sediment supply to the deeper basin. These changes in basin and pathway morphology may be related to increased rates of sea-floor spreading at 10.0 Ma [*Mosar et al.*, 2002].

The mean recurrence of Canary Island landslides over the 17 Ma period is 0.135 Ma, and over the last 7.0 Ma the mean recurrence is 0.130 Ma. Although the recurrence remains the same across these two periods, the individual turbidite volumes increase by an order of magnitude at 7.0 Ma. This increase in volume is also seen in organic-rich siliciclastic turbidites [*Lebreiro et al.*, 1998; *Weaver et al.*, 1998; *Weaver*, 2003], and therefore probably reflects a change in turbidite pathway to the deep basin, rather than a change in the scale of failure.

6.5. Turbidite Clustering

Rescaled range analysis was used to test the degree of clustering for landslide recurrence intervals, to derive the Hurst exponent, termed K [*Hurst*, 1951; *Chen and Hiscott*, 1999]. The Hurst exponent for the complete 17 to 0 Ma record ($N=124$) is $K=0.72$. The equivalent result for the last 7 Ma record ($N=58$) is $K=0.50$. Values of K greater than 0.6 within finite data sets indicate serial dependence or clustering, while values close to 0.6 indicate no dependence, and values less than 0.6 indicate that there is a negative dependence, where an increase in the independent variable causes a decrease in the dependent variable [*Wallis and Matalas*, 1970; *Chen and Hiscott*, 1999]. Turbidites that were most likely from Tenerife provenance have a mean recurrence interval of 0.27 Ma, which is similar to the mean recurrence of Late Quaternary Tenerife-sourced landslides at 0.33 Ma [*Hunt et al.*, 2013a]. The Hurst exponent of Tenerife-sourced turbidites is 0.79 ($N=25$).

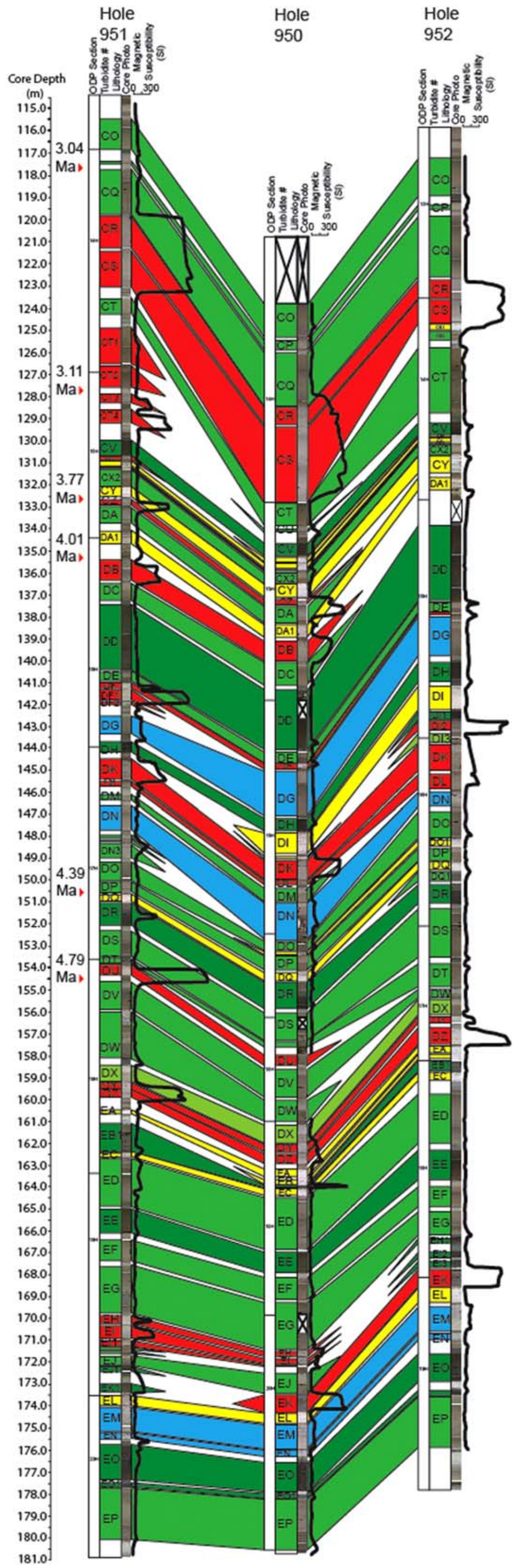

Figure 6. Correlation plot of ODP holes 950, 951, and 952 showing Early Pliocene-age turbidites in the Madeira Abyssal Plain. Dates from *Howe and Sblendorio-Levy* [1998]. Turbidite legend from Figure 4.

The Hurst exponent values indicate that the 0–17 Ma record may show a degree of clustering, which is apparent in the observed difference in landslide activity before and after ~7 Ma. Over the last 7 Ma, volcanic landslides do not show serial dependence when considered together, which means that the occurrence of a landslide is not affected by the landslide before it. Analysis of the Tenerife-sourced beds alone, however, does indicate a degree of clustering, highlighted with groupings at 6.8-5.8 Ma, 4.6-4.2 Ma, 2.6-1.7 Ma and 1.2-0.17 Ma (Figure 12). However, the sample size is below that recommended for this type of analysis (N>50) [*Chen and Hiscott*, 1999]. Given the less than optimal sample size, the results for Tenerife-source landslides should be treated with caution.

6.6. Sea Level and Landslide Frequency

To further explore controls on volcanic landslide timing a Generalized Linear Model [*Nelder and Wedderburn*, 1972] and a Proportional Hazards Model [*Cox*, 1972] were employed. Two scenarios were run to test for a statistically significant relationship between eustatic sea-level change, and its first derivative (i.e., rate of change), and landslide occurrence. Only the 7 to 0 Ma record was analyzed, as a high-resolution sea level curve exists only for this interval [*Miller et al*., 2005]. This statistical analysis provides p values, which determine whether a given null hypothesis can be rejected. Hence, if we are testing that sea level is not a significant controlling factor, then $p<0.05$ allows us to reject that hypothesis (i.e., sea level may be significant). It would not, however, prove the significance of sea level outright.

It is necessary to exclude ("censor") the time interval since the last landslide from the statistical analysis, as the time to the next event is at some undetermined point in the future. It is not necessary to censor any further data points. Hence the sample size for Tenerife-sourced landslides is N=25 and for volcanic landslides is N=37 for the last 7 Ma. Small sample sizes of N<100 are not optimal for robust statistical analyses, but *Peduzzi et al*. [1995] demonstrated that a minimum value of only ten events per variable is required for proportional hazards models. *Vittinghoff and McCulloch* [2007] proposed that this value could be relaxed even further. Given that only two variables are being tested here, this indicates a minimum sample size of N=20 may be adequate; hence the application of a Proportional Hazards Model can be justified. A mini-

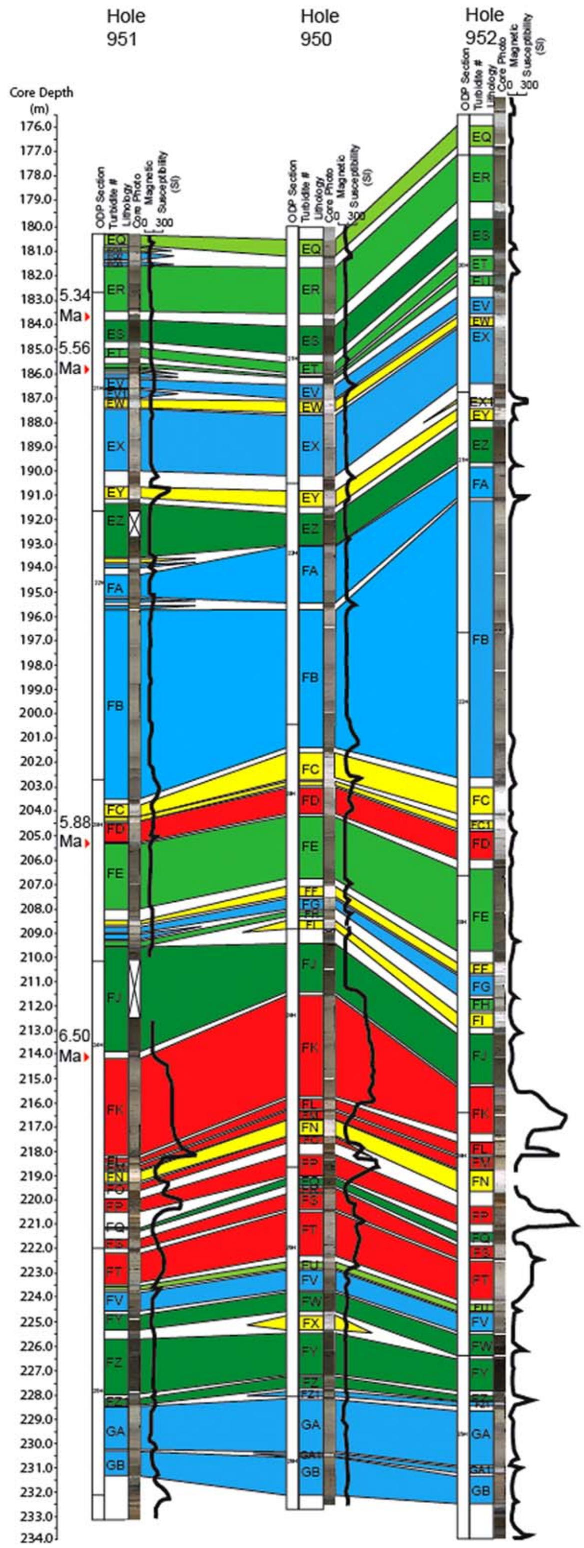

Figure 7. Correlation panel of ODP holes 950, 951, and 952 showing Late Miocen-age turbidites in the Madeira Abyssal Plain. Dates from *Howe and Sblendorio-Levy* [1998]. Turbidite legend from Figure 4.

mum sample size for the Generalized Linear Model has not been determined; therefore the results cannot be viewed with the same level of confidence.

Results of an exponential regression analysis comparing the timing of landslides with the explanatory variables (sea level or rate of sea level change) demonstrate no statistical significance, even at the 90% level (Table 3). A second analysis fitted a Generalized Linear Model with a Gamma curve (of which the exponential is a special case). The dispersion parameter (α) ranges of the fitted Gamma curves are indicative of near-exponential distributions. A true exponential distribution lacks memory [*Parzen*, 1962], such that the probability of a new event occurring is independent of the time since the last event [*Gardiner*, 2004]. There is some subtle deviation from a true exponential ($\alpha \approx 1$) in the results (Table 3; $\alpha = 0.7$–2.0), hence it might be argued that there is a weak, temporally related control rather than the distribution being purely random. That the combined turbidite record for the last 7 Ma shows the best agreement with a true exponential distribution ($\alpha \approx 1.2$) may be attributed to multiple overprinted frequency distributions from different input sources, or simply to a process that occurs randomly in time.

The final analysis (Proportional Hazards Model of *Cox* [1972] takes a different approach, and compares $h(t)$, the hazard rate with the explanatory variables. The hazard rate is the probability that an event will occur at time t given that one occurred at time $t=0$. An exponential distribution would indicate a constant hazard rate, whereas other processes have either decreasing or increasing hazard rates. This analysis assumes that hazard rate is proportional to an explanatory variable in order that its effect can be estimated. It is not necessary to determine the distribution form of recurrence intervals, which makes it a particularly valuable technique [*Smith et al*., 2003]. For this analysis, recurrence intervals were determined in two ways: time since last event (termed "post"), and time since previous event (termed "prior").

The Cox Proportional Hazards Model performs three separate statistical tests that were used to determine significance of global sea level and its first derivative. The results were not found to be significant at the

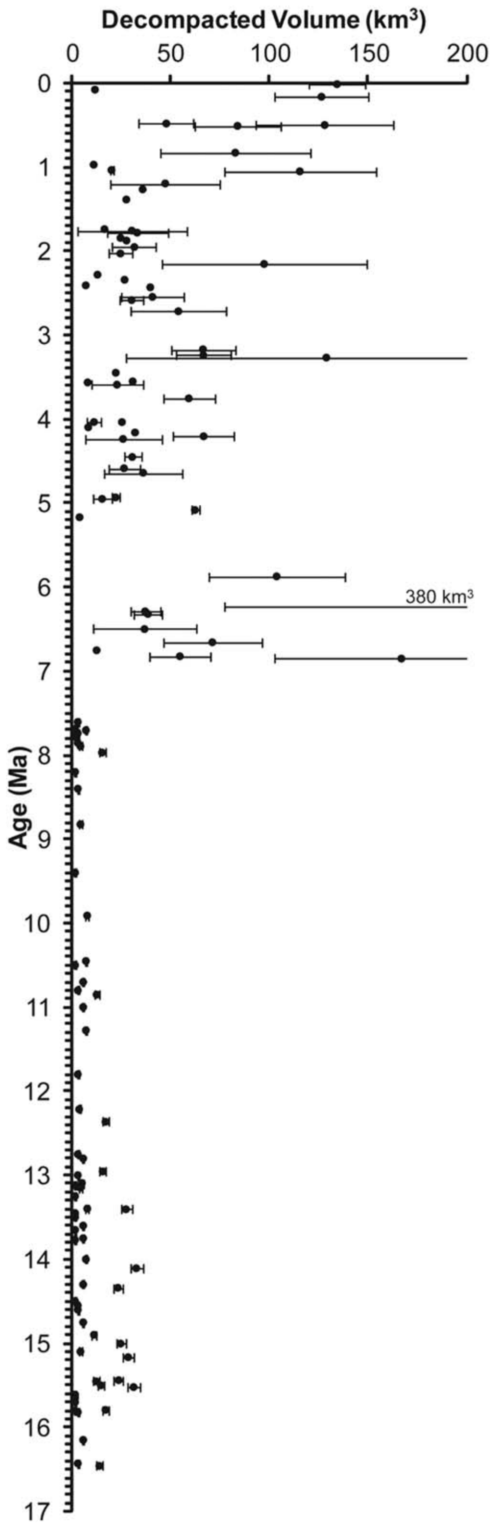

Figure 8. Graph showing decompacted volume of the volcaniclastic turbidites against the calculated age of the respective event. Error bars represent the range in volume calculated by applying *Weaver* [2003] method to each core site.

90% level (Table 3). While the sample sizes are relatively small, the fact that the statistical tests all yield similar values provides confidence in the outcome. Although the results do not show statistical significance, it is notable that the Tenerife-sourced beds show the lowest values ($p = -0.3$) in relation to sea level for the "prior" calculation; hence there may be some weak signal albeit not quantifiably significant.

It must be noted that the 7 to 0 Ma turbidite record may yield age errors as great as ± 10 ka. Calculating the ages of the beds at three independent ODP Sites provides greater confidence with age determination, however these potential age errors do invoke caution with the level of interpretation placed on the statistical relationships to sea level.

7. Discussion

7.1. Relationship of Island Collapse Turbidites With Volcanism and Denudation

7.1.1. Pre-7.0 Ma Record

The ages and trace-element depleted compositions of these beds implicate sources from the Eastern Canary Islands. Prior to this point the Western Canary Islands were yet to emerge. Indeed, there is known landslide activity dated between 14.0 and 9.0 Ma from both Gran Canaria and La Gomera [*Funck and Schmincke*, 1998; *Schmincke and Sumita*, 1998]. Furthermore, on Gran Canaria rhyolitic lavas and ash fall tuffs accumulated between 14.0 and 12.5 Ma, following by basaltic lavas and extra-caldera phonolites between 12.6 and 9.7 Ma [*McDougall and Schmincke*, 1976].

7.1.2. Mid-Late Miocene 7.0–6.0 Ma Record

Beds *FT*, *FS* and *FR* have basic compositions, while beds *FP*, *FO*, *FM*, *FL* and *FD* have compositions that implicate the evolved provenance of Tenerife, similar to the most recent *G*, *O* and *Z* turbidites (representing beds *Mg*, *Mo*, and *Mz* of *Hunt et al*. [2013a, 2013b]. The dates and compositions means that beds *FP*, *FO*, *FM*, *FL* and *FD* could represent failures of the earliest subaerial shield phases of the Anaga and Teno massifs of Tenerife (Figure 12), while beds *FT*, *FS* and *FR* were derived from the older basaltic submarine flank. During this period there is little evidence of prodigious landslides on Lanzarote, Gran Canaria or La Gomera, while La Palma and El Hierro are yet to form. Indeed, other than the Masca, Carrizales and Teno landslides from Tenerife (aged 6.65 to 6.0 Ma) there are no other major landslides documented in the Canary Islands at this time [*Walter and Schmincke*, 2002; *Acosta et al*., 2003].

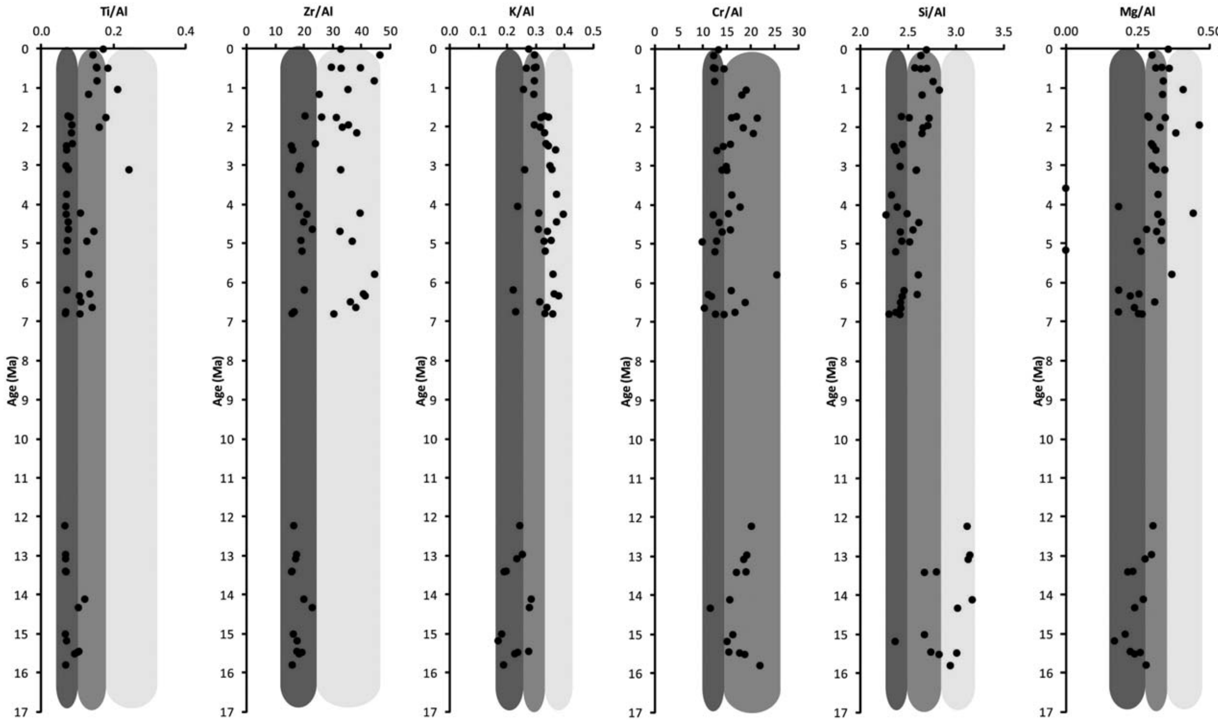

Figure 9. Carbonate-free major element composition of volcaniclastic turbidite mudcaps at hole 950 against depth, based on the *Jarvis et al*. [1998].

The voluminous early basaltic phase of shield-building on Tenerife is also the most likely source of the voluminous ~6.2 Ma bed *FK* turbidite (Figure 7). During this period there was volcanic activity on both La Gomera and early phase shield building on Tenerife (*Thirlwall et al*., 2000; *Paris et al*., 2005; *Ancochea et al*., 2006]. Bed *FK* may represent one of aforementioned Tenerife slides, and must reflect the failure of a significant proportion of the submarine flank to account for its basic composition and volume.

7.1.3. Early Pliocene 5.3–4.0 Ma Record

The largest volume turbidites (beds *EK* and *DK*) have evolved compositions, with bed *DK* having a similar composition to turbidites of Tenerife provenance. The ~4.2 Ma bed *DK* turbidite was emplaced at a similar time to the major collapse of the Anaga massif [*Krastel et al*., 2001; *Acosta et al*., 2003].

Other turbidites of this period (beds *EI*, *EH*, *DZ*, *DY*, *DU*, *DL*, and *DF*) have different basic compositions, with notably increased potassium, most likely from an older island source, such as La Gomera or Gran Canaria. *Acosta et al*. [2003] indicated that numerous relatively small-scale landslides occurred around La Gomera at ~4.0 Ma, suggesting La Gomera as the probable source for these beds. The volcanic activity on La Gomera is coincident with these smaller beds [*Paris et al*., 2005; *Ancochea et al*., 2006], while beds EK and DK coincide with earlier eruptions on Tenerife [*Van den Bogaard and Schmincke*, 1998; *Thirlwall et al*., 2000].

7.1.4. Late-Early Pliocene to Early-Late Pliocene 3.7-3.0 Ma Record

The thickest and most volumetric beds during this period are *DB* (3.75 Ma), *CS* (3.27 Ma), *CR* (3.24 Ma) and *CM* (3.17 Ma). The remaining volcaniclastic turbidites are minor thin-bedded events in the Madeira Abyssal Plain sequence. Owing to the ages, and in part the compositions, of these deposits, Gran Canaria is suggested as a possible source, since there is evidence of contemporaneous landslide activity, including the Roque Nublo and Galdar landslides [*Acosta et al*., 2003]. Indeed, the >120 km^3 bed CS is linked to the Roque Nublo landslide. The Roque Nublo stratocone was built between 5.0 and 3.5 Ma, with explosive terminal phase eruptions [*Anguita et al*., 1991]. The later phases of this volcanic activity are synchronous with these turbidites.

7.1.5. Late Pliocene 2.8-1.8 Ma Record

This time period commenced with beds *BZ*, *BQ* and *BN* (Figure 5). The 2.7 to 2.5 Ma ages and compositions of beds *BZ* and *BQ* would implicate Gran Canaria or La Gomera as the source. From 2.7 to 2.5 Ma there was

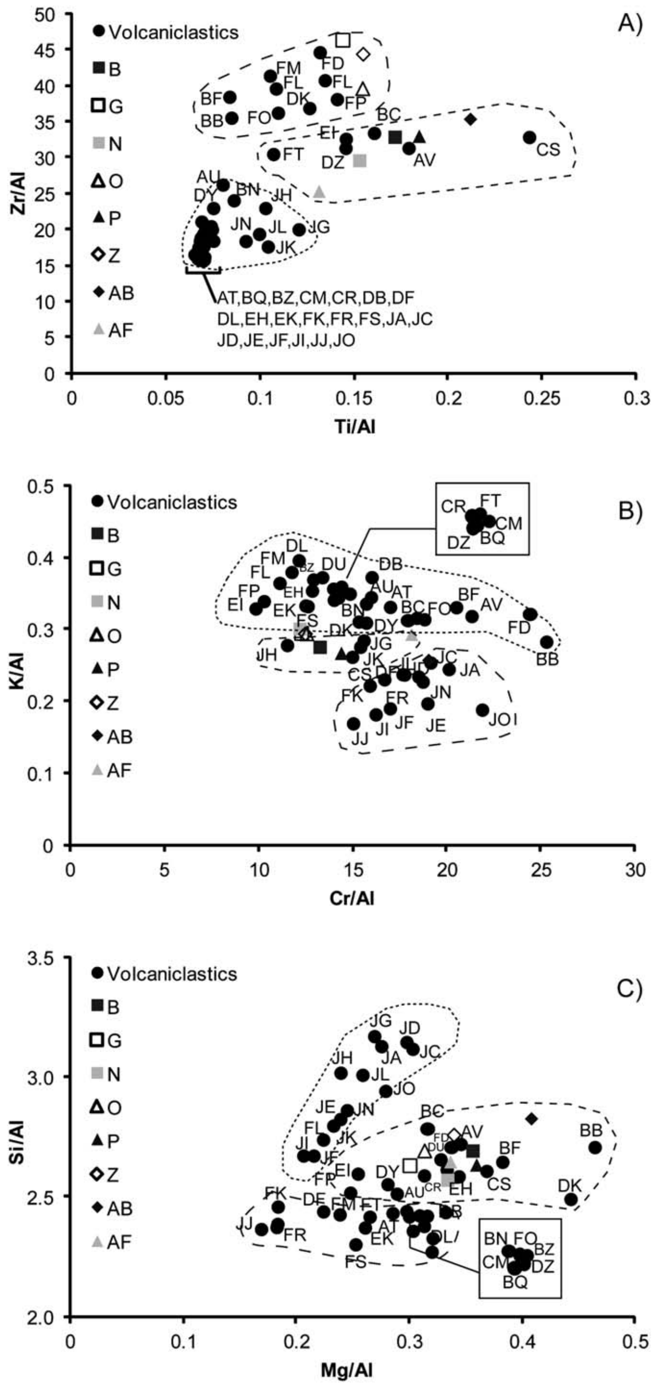

Figure 10. Cross plots of mudcap geochemistry of the volcaniclastic turbidites sampled at hole 950 showing delineation of composition fields. (a) Zr/Al against Ti/Al, (b) K/Al against Cr/Al, and (c) Si/Al against Mg/Al. The highlighted turbidites in the legend are the Quaternary turbidites discussed in *Hunt et al.* [2013a].

volcanic activity on Tenerife and Gran Canaria (Figure 12), with a cessation of activity on La Gomera [*McDougall and Schmincke*, 1976; *Paris et al.*, 2005; *Ancochea et al.*, 2006]. Beds *AV* and *AU* have basic compositions with moderate-to-high K and Mg, similar to those ascribed to a La Palma or El Hierro provenance, but were deposited at a time before El Hierro had emerged. However, volcanic activity commenced on La Palma toward the end of this time period [*Ancochea et al.*, 1994], so La Palma presents a viable source for these later turbidites.

The voluminous bed BF, dated at 2.2 Ma, has an evolved composition similar to those previously ascribed to a Tenerife source, and could represent the Tigaiga landslide, which has been dated at 2.3 Ma [*Cantagrel et al.*, 1999]. As with similar Tenerife sourced events from the 1.5 Ma to recent turbidite record, this Tigaiga landslide coincided with terminal eruptions of a volcanic cycle (mafic Lower Group, dated at 3.5-2.1 Ma by *Ablay and Marti* [2000]). Lastly, beds *BC* and *BB* have a similar composition to bed BF, and may represent a subsequent failure of the northern flank of Tenerife at ∼1.95 Ma.

7.1.6. The 1.5 Ma to Recent Record

Beds *B* (∼15 ka), *P* (0.54 Ma) and *AB* (1.05 Ma) have a provenance from El Hierro, and can be assigned to the El Golfo, El Julán and El Tiñor landslides respectively [*Hunt et al.*, 2013a]. It is proposed that bed *N* (0.49 Ma) originated from La Palma, and is potentially associated with the Cumbre Nueva landslide. Beds *G* (0.165 ka), *O* (0.535 ka), *Z* (0.84 ka) and *AF* (∼1.2 Ma) are attributed to a Tenerife source, due to the greater evolved composition. Given the ages of these beds, they are interpreted to represent the Icod, Orotava, Güímar, and Roques de García landslides respectively [*Hunt et al.*, 2013a].

7.2. Landslide Preconditioning Factors and Triggers

The chronology and provenance of the volcaniclastic turbidites in the Madeira Abyssal Plain, coupled with onshore dates of known Canary Island landslides, can help understand landslide preconditioning factors and triggers. However, it must be noted that the turbidites in the Madeira Abyssal Plain represent only the

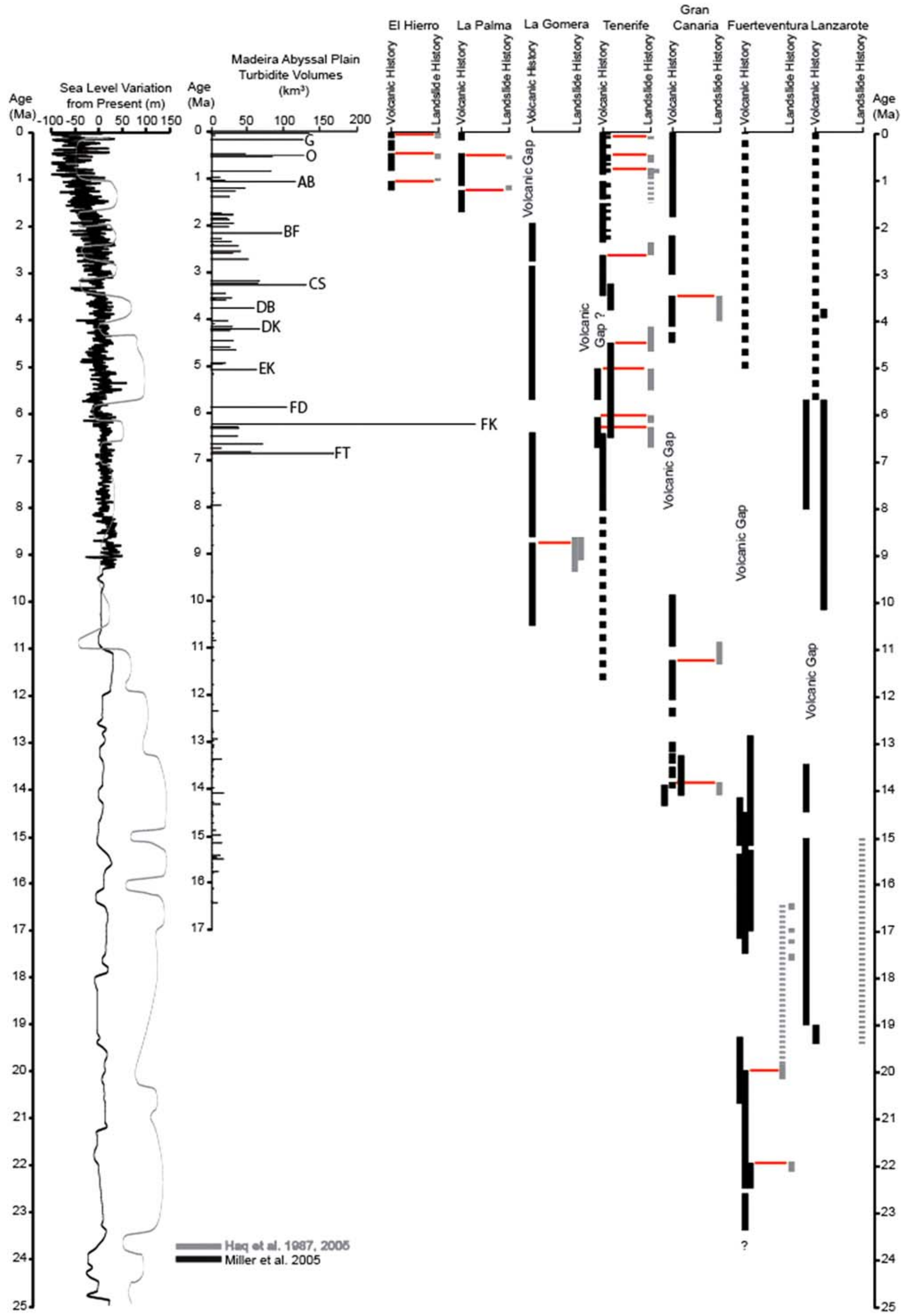

Figure 11. Summary of volcanic activity on the Canary Islands (black bars) and onshore landslide evidence (gray bars); compared to the volcaniclastic turbidite history and the *Miller et al.* [2005] sea level curve. Inlay shows comparison of high resolution 0–7 Ma sea level record against the occurrence of voluminous volcaniclastic turbidites. The red lines represent landslides potentially linked to failures at the end of volcanic cycles.

largest flank collapses in the Canary Islands (>5 km^3 and commonly >100 km^3), with smaller failures most likely not capable of producing such long-runout turbidity currents. Furthermore, it is assumed that all large flank collapses were disintegrative and able to produce an associated sediment gravity flow, and that the landslides neither aborted nor failed to produce a turbidity current [*Day et al*., 1997]. A last assumption is that the sediment gravity flows produced were routed to the Madeira Abyssal Plain, and were not restricted to local depocentres.

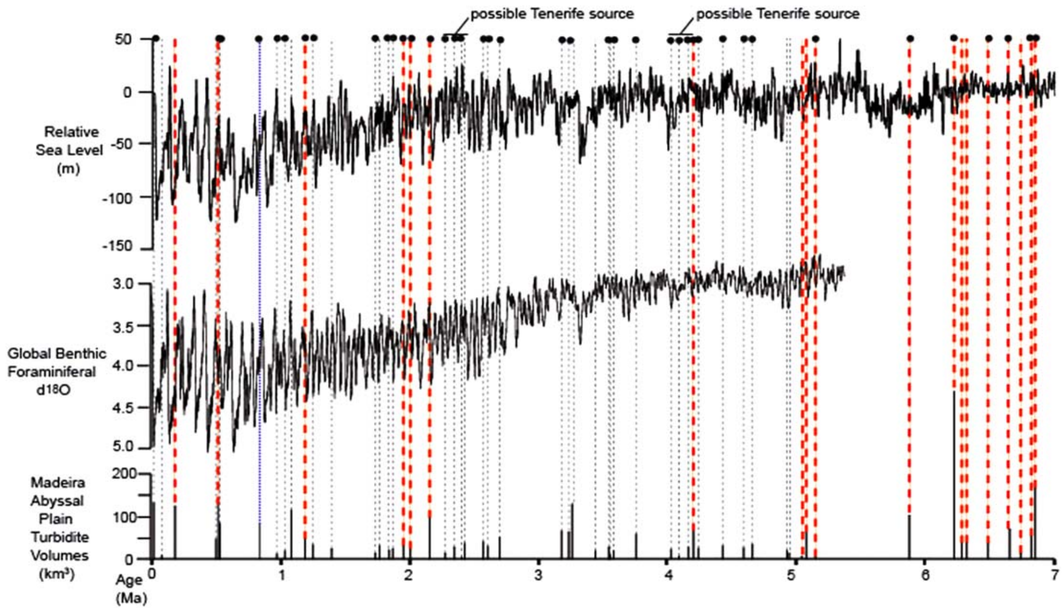

Figure 12. Summary of volcanic turbidite occurrence with magnitude against records of climate [*Lisieki and Raymo*, 2005] and sea level [*Miller et al.*, 2005]. Gray-dashed lines present volcanic island-sourced turbidites, while the red-dashed lines represent specifically Tenerife-sourced turbidites. The events capped with a closed black circle signify those events proposed to correlate with rising or highstands of sea level.

The turbidites from this study contain large volumes that may be excess to those reported for the associated onshore landslide scar. Accurate onshore scar volumes may be difficult to calculate due to thicknesses of infilled volcanic materials. It has been demonstrated that significant components of the submarine flank could have contributed to the landslide, and thus turbidite, volume, and therefore account for the excessive volumes [*Hunt et al.*, 2011]. Although estimates from the Icod landslide deposit suggest that only around 10% of the turbidite volume originates from seafloor erosion by the slide or turbidity current [*Hunt et al.*, 2011], this assumption cannot be made confidently for the other slides; thus seafloor erosion could account for the excessive turbidite volumes. Although turbidite volumes are provided in this study, there are many assumptions that affect how this volume reflects the true magnitude of the initial failure. Therefore this study focuses on the provenance, timing and recurrence of the landslides, with only qualitative reference to deriving landslide magnitude from the turbidite volume.

With these assumptions noted, a relatively complete record of Canary Island landslide activity is available for investigation. First, there is no serial dependence between the occurrences of volcanic island landslides over the last 17 Ma, and over the last 7 Ma in particular, so that events are not strongly clustered in time. However, the results of Tenerife-sourced turbidites suggest that there may be a subtle degree of temporal clustering. Large-volume landslides commonly occur during periods of volcanism on the respective islands,

Table 3. Summary of Statistical Analysis[a]

Sample	Explanatory Variable	Exponential Regression (p)	GLM (Dispersion Parameter, α)	PHM (Results for Prior/Post) Likelihood Test [p]	Wald Test [p]	Logrank Test [p]
0–7 Ma all turbidites	Sea Level	0.40	1.21	0.700/0.503	0.500/0.699	0.500/0.699
	First Derivative of Sea Level	0.49	1.19	0.637/0.704	0.624/0.684	0.624/0.684
0–7 Ma volcanic landslides	Sea Level	0.84	0.70	0.604/0.663	0.610/0.668	0.610/0.668
	First Derivative of Sea Level	0.74	0.75	0.895/0.879	0.910/0.873	0.914/0.873
0–7 Ma Tenerife-sourced landslides	Sea Level	0.21	2.02	0.296/0.814	0.305/0.815	0.302/0.815
	First Derivative of Sea Level	0.21	1.68	0.504/0.872	0.535/0.893	0.521/0.892

[a]Neither sea level nor its first derivative are found to be a statistically significant control on landslide timing (exponential regression and Generalized Linear Model, GLM) or hazard rate (Proportional Hazards Model, PHM).

rather than periods of volcanic quiescence (Figures 11 and 12). However, volcanic sequences are often sparsely dated and often limited to the largest events, and thus there are uncertainties and a relationship between landslide occurrence and volcanism cannot be statistically evaluated. The limited evidence of this study can at least suggest that loading of the volcanic edifice and related seismicity can be inferred to be preconditioning factors for collapse of the island flanks; however, the strength of this relationship and the exact contribution cannot be resolved.

Previously, it has been inferred that warm and wet climates, associated with the transition from glacial lowstand conditions to interglacial highstand conditions, are associated with flank collapses in the Hawaiian archipelago [*McMurtry et al*., 2004]. Seventy percent of 7 Ma to recent volcaniclastic turbidites in the Madeira Abyssal Plain ($>$5 km^3) occur at periods of rising sea level or relative highstands of sea level (Figures 11 and 12). However, our statistical analysis provides no support for a correlation between the collapse turbidite occurrence and sea-level change. We may consider that if an environmental control is operating, then it is either weak (and therefore not proven by the statistical analysis) or there may be a dynamic interrelationship between multiple controlling variables (e.g., sea level, climate, weathering, unroofing processes). It is worth noting that many processes, such as development of overpressure and temperature may not operate immediately in response to changes in sea level.

This trend showing a weak or nonsignificant correlation of submarine landslide occurrence with climate change is being found in an increasing number of study areas. Indeed, the 600 ka to recent record of continental slope-derived turbidites in Agadir Basin demonstrates a Poisson-like process as the trigger mechanism, demonstrating a reduced influence of climate [*Hunt et al*., 2013c].

8. Conclusions

ODP Cores in the Madeira Abyssal Plain contain a record of $>$100 volcanic island landslides over the last 17 Ma. Large-volume volcaniclastic landslides occurred mainly after 7 Ma, and are represented by metre-thick turbidites. Mudcap geochemistry and biostratigraphic dating of these turbidites has provided an important long-time record of volcanic island flank collapse in the Canary Islands, that can be tied make to proximal landslide histories. This ODP record provides one of the most extensive archives of landslide activity from a volcanic archipelago. The mean landslide recurrence interval is 0.130–0.135 Ma. Moreover, the record has allowed landslides from particular islands to be potentially identified, for example landslides from Tenerife have a mean recurrence of $\sim$0.3 Ma.

There is a potential coincidence of turbidite occurrence with periods of protracted intrusive and extrusive volcanism on the respective island. However, the strength of this particular correlation cannot be tested. Furthermore, the exact preconditioning and/or trigger factor associated with volcanism that could instigate landsliding cannot be accurately resolved.

Statistical analysis of landslide recurrence and global eustatic sea level fails to demonstrate any statistical significance even at the 90% level of statistical significance. This study presents an excellent record of volcaniclastic turbidites with good biostratigraphic dating, and it suggests that sea level plays only a minor role in causing large-scale collapses in the Canary Islands. This is important because it is predicted that sea level may rise rapidly in the near future.

Acknowledgments
The authors would like to thank the scientists and crew that worked on the original ODP Leg 157 core recovery. JEH would like to acknowledge the PhD funding from Marine Geoscience Group at NOCS that aided completion of this work. Analytical work by IJ was funded by NERC ODP grant GST/02/1097. I would also like to thank two anonymous reviewers and editor Roger Urgeles for their invaluable input to this work.

References

Ablay, G. J., and M. Hürlimann (2000), Evolution of the north flank of Tenerife by recurrent giant landslides, *J. Volcanol. Geotherm. Res.*, *103*, 135–159.

Ablay, G. J., and J. Marti (2000), Stratigraphy, structure and volcanic evolution of the Pico-Teide Viejo formation, Tenerife, Canary Islands, *J. Volcanol. Geotherm. Res.*, *103*(1-4), 183–208.

Acosta, J., E. Uchupi, A. Muñoz, P. Herranz, C. Palomo, M. Ballesteros, and ZEE Working Group (2003), Geologic evolution of the Canary Islands of Lanzarote, Fuerteventura, Gran Canaria and La Gomera and comparison of the landslides at these islands with those at Tenerife, La Palma and El Hierro, *Mar. Geophys. Res.*, *24*, 1–40, doi:10.1007/s11001-004-1513-3.

Alibés, B., M. Canals, B. Alonso, S. M. Lebreiro and P. P. E. Weaver (1996), Quantification of Neogene and Quaternary sediment input to the Madeira Abyssal Plain, *Geogaceta*, *20* (2), 394–397.

Alibés, B., R. G. Rothwell, M. Canals, P. P. E. Weaver and B. Alonso (1999), Determination of sediment volumes, accumulation rates and turbidite emplacement frequencies on the Madeira Abyssal Plain (NE Atlantic): A correlation between seismic and borehole data, *Mar. Geol.*, *160*(3-4), 225–250.

Ancochea, E., J. M. Fúster, E. Ibarrola, A. Cendrero, J. Coello, F. Hernán, J. M. Cantagrel, and C. Jamond (1990), Volcanic evolution of the island of Tenerife (Canary Islands) in the light of new K-Ar data, *J. Volcanol. Geotherm. Res.*, *44*, 231–249.

Ancochea, E., F. Hernán, A. Cendrero, J. M. Cantagrel, J. M. Fúster, E. Isbarrola, and J. Coello (1994), Constructive and destructive episodes in the building of a young Ocean Island, La Palma, Canary Islands, and the genesis of the Caldera de Taburiente, *J. Volcanol. Geotherm. Res.*, *60*(3-4), 243–262.

Ancochea, E., M. J. Huertas, J. M. Cantagrel, J. Coello, J. M. Fúster, N. Arnaud, and E. Ibarrola (1999), Evolution of the Cañadas edifice and its implications for the origin of the Cañadas Caldera (Tenerife, Canary Islands), *J. Volcanol. Geotherm. Res.*, *88*(3), 177–199.

Ancochea, E., F. Hernán, M. J. Huertas, J. L. Brändle, and R. Herrera (2006), A new chronostratigraphy and evolutionary model of La Gomera: Implications for the overall evolution of the Canarian Archipeligo, *J. Volcanol. Geotherm. Res.*, *157*(4), 271–293.

Andrade, S. D., and B. van Wyk de Vries (2010), Structural analysis of the early stages of catastrophic stratovolcano flank-collapse using analogue models, *Bull. Volcanol.*, *72*, 771–789.

Anguita, F., and F. Hernán (1990), The Canary Islands origin: A unifying model, *J. Volcanol. Geotherm. Res.*, *103*(1-4), 1–26.

Anguita, F., L. García Cacho, F. Colombo, A. González Camacho, and R. Vieira (1991), Roque Nublo caldera: A new stratocone caldera in Gran Canaria, Canary Islands, *J. Volcanol. Geotherm. Res.*, *47*(1-2), 45–63.

Athy, L. F. (1930), Density, porosity, and compaction of sedimentary rocks, *AAPG Bull.*, *14*, doi:10.1306/3D93289E-16B1–11D7–8645000102C1856D.

Baldwin, B., and C. O. Butler (1985), Compaction curves, *AAPG Bull.*, *69*, 622–626, doi:10.1306/AD462547-16F7–11D7–8645000102C1865D.

Cantagrel, J. M., N. O. Arnaud, E. Ancochea, J. M. Fúster, and M. J. Huertas (1999), Repeated debris avalanches on Tenerife and genesis of Las Cañadas caldera wall (Canary Islands), *Geology*, *27*(8), 739–742.

Carey, S., T. Maria, and W. Cornell (1998), Processes of volcaniclastic sedimentation during the early growth stages of Gran Canaria based on sediments from Site 953, in *Proceedings of the Ocean Drilling Program, Scientific Results*, vol. 157, edited by P. P. E. Weaver, et al., pp. 183–200, Ocean Drill. Program, College Station, Tex.

Carracedo, J. C. (1994), The Canary Islands: An example of structural control on the growth of large oceanic-island volcanoes, *J. Volcanol. Geotherm. Res.*, *60*(3), 225–241.

Carracedo, J. C. (1999), Growth, structure, instability and collapse of Canarian volcanoes and comparisons with Hawaiian volcanoes, *J. Volcanol. Geotherm. Res.*, *94*(1), 1–19.

Carracedo, J. C., S. J. Day, H. Guillou, E. Rodríguez Badiola, J. A. Canas and F. J. Pérez Torrado (1998), Hotspot volcanism close to a passive continental margin: The Canary Islands, *Geol. Mag.*, *135*(5), 591–604.

Carracedo, J. C., S. J. Day, H. Guillou, and F. J. Pérez Torrado (1999), Giant quaternary landslides in the evolution of La Palma and El Hierro, Canary Islands, *J. Volcanol. Geotherm. Res.*, *94*, 169–190.

Carracedo, J. C., E. Rodríguez Badiola, H. Guillou, J. de la Nuez, and F. J. Pérez Torrado (2001), Geology and volcanology of La Palma and El Hierro (Canary Islands), *Estudios Geológicos*, *57*, 175–273.

Chen, C., and R. N. Hiscott (1999), Statistical analysis of facies clustering in submarine fan turbidite successions, *J. Sediment Res.*, *69*(2), 505–517.

Clouard, V., A. Bonneville, and P.-Y. Gillot (2001), A giant landslide on the southern flank of Tahiti Island, French Polynesia, *Geophys. Res. Lett.*, *28*(11), 2253–2256.

Cox, D. R. (1972), Regression models and life-tables, *J. R. Stat. Soc., Ser. B*, *34*(2), 187–220.

Day, S. J. (1996), Hydrothermal pore-fluid pressure and the stability of porous, permeable volcanoes, in *Volcano Instability on the Earth and Other Planets, Geol. Soc. Spec. Publ.*, vol. 110, edited by W. J. McGuire, A. P. Jones, and J. Neuberg, pp 77–94, Geol. Soc. of London, London, U. K.

Day, S. J., J. C. Carracedo, and H. Guillou (1997), Age and geometry of an aborted rift flank collapse: The San Andreas fault system, El Hierro, Canary Islands, *Geol. Mag.*, *134*(04), 523–537.

Deeming, K. R., B. McGuire and P. Harrop (2010), Climate factors of volcano lateral collapse: Evidence from Mount Etna, Sicily, *Philos. Trans. R. Soc. A.*, *368*(1919), 2559–2577, doi:10.1098/rsta.2010.0054.

De Lange, G. J., I. Jarvis and A. Kuijpers (1987), Geochemical characteristics and provenance of late Quaternary sediments from the Madeira Abyssal Plain, N Atlantic, in *Geology and Geochemistry of Abyssal Plains, Geol. Soc. Spec. Publ.*, vol. 31, edited by P. P. E. Weaver and J. Thomson, pp 147–165, Geol. Soc. Publ. House, Bath, U. K.

Deplus, C., A. Le Friant, G. Boudon, J.-C. Komorowski, B. Villemant, C. Harford, J. Ségoufin, and J.-C. Cheminée (2001), Submarine evidence for large-scale debris avalanches in the Lesser Antilles Arc, *Earth Planet. Sc. Lett.*, *192*(2), 145–157.

Edgar, C. J., J. A. Wolff, P. H. Olin, H. J. Nichols, A. Pittari, R. A. F. Cas, P. W. Reiners, T. L. Spell, and J. Marti (2007), The late Quaternary Diego Hernandez Formation, Tenerife: Volcanology of a complex cycle of voluminous explosive phonolitic eruptions, *J. Volcanol. Geotherm. Res.*, *160*(1), 59–85.

Elsworth, D., and S. J. Day (1999), Flank collapse triggered by intrusions: The Canarian and Cape Verde Archipelagos, *J. Volcanol. Geotherm. Res.*, *94*, 323–340.

Elsworth, D., and B. Voight (2001), The mechanics of harmonic gas pressurization and failure of lava domes, *Geophys. J. Int.*, *145*, 187–198, doi:10.1111/j.1365-246X.2001.00370.x.

Fine, I. V., A. B. Rabinovich, R. E. Thomson, and E. A. Kulikov (2003), Numerical modelling of tsunami generation by submarine and subaerial landslides, 69–88, in *Submarine Landslides and Tsunamis*, edited by A. C. Yalçiner, E. Pelinovsky, and C. E. Synolakis, Kluwer Acad., Netherlands.

Frenz, M., R. B. Wynn, A. Georgiopoulou, V. B. Bender, G. Hough, D. G. Masson, P. J. Talling, and B. Cronin (2009), Provenance and pathways of late Quaternary turbidites in the deep-water Agadir Basin, northwest African margin, *Int. J. Earth Sci.*, *98*(4), 721–733.

Fritz, H. M., F. Mohammed, and J. Yoo (2009), Lituya Bay landslide impact generated mega-tsunami 50th Anniversary, *Pure App. Geophys.*, *166*(1-2), 153–175, doi:10.1007/s00024-008-0435-4.

Funck, T., and H.-U. Schmincke (1998), Growth and destruction of Gran Canaria deduced from seismic reflection and bathymetric data, *J. Geophys. Res.*, *103*(B7), 15393–15407.

Garcia, M. O. (1996), Turbidites from slope failure of Hawaiian volcanoes, in *Volcano Instability on the Earth and other Planets, Geol. Soc. Spec. Publ.*, vol. 110, edited by W. J. McGuire, A. P. Jones, and J. Neuberg, pp. 281–294, Geol. Soc., London, U. K.

García Cacho, L., J. L. Díez-Gil, and V. Araña (1994), A large volcanic debris avalanche in the Pliocene Roque Nublo Stratovolcano, Gran Canaria, Canary Islands, *J. Volcanol. Geotherm. Res.*, *63*(3-4), 217–229.

Garcia, M. O., and Hull, D. M. (1994), Turbidites from giant Hawaiian landslides: Results from Ocean Drilling Program Site 842, *Geology*, *22*, 159–162.

Gardiner, C. W. (2004), *Handbook of Stochastic Methods: For Physics, Chemistry, and the Natural Sciences*, 3rd ed., Springer-Verlag, Berlin, Heidelberg.

Gee, M. J., A. B. Watts, D. G. Masson, and N. C. Mitchell (2001), Landslides and the evolution of El Hierro in the Canary Islands, *Mar. Geol.*, *177*, 271–293.

Giachetti, T., R. Paris, K. Kelfoun, and F. J. Pérez-Torrado (2011), Numerical modelling of the tsunami triggered by the Güímar debris avalanche, Tenerife (Canary Islands): Comparison with field-based data, *Mar. Geol.*, *284*, 189–202.

Goldstrand, P. M. (1998), Provenance and sedimentologic variations of turbidite and slump deposits at Sites 955 and 956, in *Proceedings of the Ocean Drilling Program, Scientific Results*, vol. 157, edited by P. P. E. Weaver et al., pp. 343–360, Ocean Drill. Program, College Station, Tex.

Guillou, H., J. C. Carracedo, C. Laj, C. Kissel, F. Perez Torrado, and E. Rodriguez Badiola (1995), K-Ar ages and geomagnetic reversals from lavas of Hierro, Canary Islands, *Tierra Nova*, *7*, 163.

Harris, P. D., M. J. Branney, and M. Storey (2011). Large eruption-triggered ocean-island landslide at Tenerife: Onshore record and long-term effects on hazardous pyroclastic dispersal, *Geology*, *39*(10), 951–954.

Haq, B. U., and A. M. Al-Qahtani (2005), Phanerozoic cycles of sea-level change on the Arabian Platform, *GeoArabia*, *10*(2), 127–160.

Haq, B. U., J. Hardenbol, and P. R. Vail (1987), Chronology of fluctuating sea levels since the Triassic, *Science*, *235*, 1156–1166.

Hildenbrand, A., P.-Y. Gillot, and A. Bonneville (2006), Offshore evidence of a huge landslide of the northern flank of Tahiti-Nui (French Polynesia), *Geochem. Geophys. Geosyst.*, *7*, Q03006, doi:10.1029/2005GC001003.

Hoernle, K., and H.-U. Schmincke (1993), The role of partial melting in the 15 Ma geochemical evolution of Gran Canaria: A blob model for the Canary hotspot, *J. Petrol.*, *34*(3), 599–626.

Hoernle, K. A. J. (1998), Geochemistry of Jurassic oceanic crust beneath Gran Canaria (Canary Islands): Implications for crustal recycling and assimilation, *J. Petrol.*, *39*(5), 859–880.

Holcomb, R. T., and R. C. Searle (1991), Large landslides from oceanic volcanoes, *Mar. Geotech.*, *10*, 19–32.

Howe, R. W., and J. Sblendorio-Levy (1998), Calcareous nannofossil biostratigraphy and sediment accumulation of turbidite sequences on the Madeira Abyssal Plain, ODP Sites 950–952, in *Proceedings of Ocean Drilling Program, Scientific Results*, vol. 157, edited by P. P. E. Weaver et al., pp. 501–515, Ocean Drill. Program, College Station, Tex., doi:10.2973/odp.proc.sr.157.129.1998.

Hunt, J. E., R. B. Wynn, D. G. Masson, P. J. Talling, and D. A. H. Teagle (2011), Sedimentological and geochemical evidence for multistage failure of volcanic island landslides: A case study from Icod landslide on north Tenerife, *Geochem. Geophys. Geosyst.*, *12*, Q12007, doi:10.1029/2011GC003740.

Hunt, J. E., R. B. Wynn, P. J. Talling, and D. G. Masson (2013a), Turbidite record of frequency and source of large volume (>100 km^3) Canary Island landslides in the last 1.5 Ma: Implications for landslide triggers and geohazards, *Geochem. Geophys. Geosyst.*, *14*, 2100–2123, doi:10.1002/ggge.20139.

Hunt, J. E., R. B. Wynn, P. J. Talling, and D. G. Masson (2013b), Multistage collapse of eight Western Canary Island landslides in the last 1.5 Ma: Sedimentological and geochemical evidence from subunits in submarine flow deposits, *Geochem. Geophys. Geosyst.*, *14*, 2159–2181,doi:10.1002/ggge.20138.

Hunt, J. E., R. B. Wynn, P. J. Talling, and D. G. Masson (2013c), Frequency and timing of landslide-triggered turbidity currents within the Agadir Basin, offshore NW Africa: Are there associations with climate change, sea level change and slope sedimentation rates?, *Mar. Geol.*, *346*, 274–291.

Hürlimann, M., E. Turon, and J. Marti (1999a), Large landslides triggered by caldera collapse events in Tenerife, Canary Islands, *Phys. Chem. Earth, Part A*, *24*(10), 921–924.

Hürlimann, M., A. Ledesma, and J. Marti (1999b), Conditions favouring catastrophic landslides on Tenerife (Canary Islands), *Terra Nova*, *11*, 106–111.

Hürlimann, M., E. Turon, and J. Marti (1999c), Large landslides triggered by caldera collapse events in Tenerife, Canary Islands, *Phys. Chem. Earth, Part A*, *24*(10), 921–924.

Hürlimann, M., Garcia-Pieram J. O., and Ledesma, A. (2000), Causes and mobility of large volcanic landslides: Application to Tenerife, Canary Islands, *J. Volcanol. Geotherm. Res.*, *22*, 163–197.

Hürlimann, M., A. Ledesma, and J. Marti (2001), Characterisation of a volcanic residual soil and its implications for large landslide phenomena: Application to Tenerife, Canary Islands, *Eng. Geol.*, *59*, 115–132.

Hürlimann, M., J. M Marti, and A. Ledesma (2004), Morphological and geological aspects related to large slope failures on oceanic islands: The huge La Orotava landslides on Tenerife, Canary Islands, *Geomorphology*, *62*(3-4), 143–158.

Hurst, H. E. (1951), Long term storage capacity of reservoir, *Am. Soc. Civ. Eng.*, *116*, 770–808.

Jarvis, I. (2003), Sample preparation for ICP-MS, in *Handbook of Inductively Coupled Plasma Mass Spectrometry*, edited by K. E. Jarvis, A. L. Gray, and R. S. Houk, pp. 172–224, Viridian, Woking, U. K.

Jarvis, I., J. Moreton, and M. Gérard (1998), Chemostratigraphy of Madeira Abyssal Plain Miocene-Pleistocene turbidites, Site 950, in *Proceedings of Ocean Drilling Program, Scientific Results*, vol. 157, edited by P. P. E. Weaver et al., pp. 535–558, Ocean Drill. Program, College Station, Tex., doi:10.2973/odp.proc.sr.157.129.1998.

Keating, B. H., and W. J. McGuire (2004), Instability and structural failure at volcanic ocean islands and the climate change dimension, *Adv. Geophys.*, *47*, 175–271.

Klitgort, K. D., and H. Schouten (1986), Plate kinematics of the central Atlantic, in *The Geology of North America,* vol. M*, The Western North Atlantic Region*, edited by P. R. Vogt and B. E. Tucholke, pp. 351–377, Geol. Soc. of Am., Boulder, Colo.

Krastel, S., H.-U. Schmincke, C. L. Jacobs, R. Rihm, T. P. Le Bas, and B. Alibés (2001), Submarine landslides around the Canary Islands, *J. Geophys. Res.*, *106*(B3), 3977–3997.

Kulikov, E. A., A. B. Rabinovich, R. E. Thomson, and B. D. Bornhold (1996), The landslide tsunami of November 3, 1994, Skagway harbor, Alaska, *J. Geophys. Res.*, *101*(C3), 6609–6615.

Lebas, E., A. Le Friant, G. Boudon, S. F. L. Watt, P. J. Talling, N. Feuillet, C. Deplus, Christian Berndt, and M. E. Vardy (2011), Multiple widespread landslides during the long-term evolution of a volcanic island: Insights from high-resolution seismic data, Montserrat, Lesser Antilles, *Geochem. Geophys. Geosyst.*, *12*, Q05006, doi:10.1029/2010GC003451.

Le Bas, T. P., D. G. Masson, R. Holtom, and I. Grevemeyer (2007), Slope failures of the flanks of the southern Cape Verde Islands, in *Submarine Mass Movements and their Consequences, Adv. in Nat. and Technol. Hazard Res.*, vol. 27, edited by V. Lykousis, D. Sakellariou, and J. Locat, pp. 337–346, Springer, Dordrecht, Netherlands.

Lebreiro, S. M., P. P. E. Weaver, and R. W. Howe (1998), Sedimentation on the Madeira Abyssal Plain: The history of turbidite infill, in *Proceedings of Ocean Drilling Program, Scientific Results*, vol. 157, edited by P. P. E. Weaver et al., pp. 523–531, Ocean Drill. Program, College Station, Tex., doi:10.2973/odp.proc.sr.157.129.1998.

Leonhardt, R., and H. C. Soffel (2006), The growth, collapse and quiescence of Teno volcano, Tenerife: New constraints from paleomagnetic data, *Int. J. Earth Sci.*, *95*(6), 1053–1064, doi:10.1007/s00531-006-0089-3.

Lisiecki, L. E., and M. E. Raymo (2005), A Pliocene-Pleistocene stack of 57 globally distributed benthic δ18O records, *Paleoceanography*, *20*(1).

Llanes, P., A. Muñoz, A. Muñoz-Martín, J. Acosta, P. Herranz, A. Carbó, and C. Palom (2003), Morphological and structural analysis in the Anaga offshore massif, Canary Islands: Fractures and debris avalanches relationships, *Mar. Geophys. Res.*, *24*(1-2), 91–112.

Llanes, P., R. Herrera, M. Gómez, A. Muñoz, J. Acosta, E. Uchupi, and D. Smith (2009), Geological evolution of the volcanic island La Gomera, Canary Islands, from analysis of its geomorphology, *Mar. Geol.*, *264*, 123–139.

Longpré, M.-A., V. R. Troll, T. R. Walter, and T. H. Hansteen (2009), Volcanic and geochemical evolution of the Teno massif, Tenerife, Canary Islands: Some repercussions of giant landslides on ocean island magmatism, *Geochem. Geophys. Geosyst.*, *10*, Q12017, doi:1029/2009GC002892.

Longpré, M.-A., J. P. Chadwick, J. Wijbrans, and R. Iping (2011), Age of the El Golfo debris avalanche, El Hierro (Canary Islands): New constraints from laser and furnace $^{40}Ar/^{39}Ar$ dating, *J. Volcanol. Geotherm. Res.*, *203*(1-2), 76–80.

Mader, C. L. (2001), Modelling the La Palma landslide tsunami, *Science of Tsunami Hazards*, *19*, 150–170.

Martí, J., and A. Gudmundsson (2000), The Las Cañadas caldera (Tenerife, Canary Islands): an overlapping collapse caldera generated by magma-chamber migration, *J. Volcanol. Geotherm. Res.*, *103*(1), 161–173.

Masson, D. G. (1994), Late quaternary turbidity current pathways to the Madeira Abyssal Plain and some constraints on turbidity current mechanisms, *Basin Res.*, *6*, 17–33.

Masson, D. G. (1996), Catastrophic collapse of the volcanic island of Hierro 15 ka ago and the history of landslides in the Canaries, *Geology*, *24*, 231–234, doi:10.1130/0091–7613(1996)024<0231:CCOTVI>2.3.CO;2.

Masson, D. G., A. B. Watts, M. R. J. Gee, R. Urgeles, N. C. Mitchell, T. Le Bas, and M. Canals (2002), Slope failures on the flanks of the western Canary Islands, *Earth Sci. Rev.*, *57*, 1–35.

Masson, D. G., C. B. Harbitz, R. B. Wynn, G. Pedersen, and F. Løvholt (2006), Submarine landslides: Processes, triggers and hazard prediction, *Philos. Trans. R. Soc. A*, *364*, 2009–2039, doi:10.1098/rsta.2006.1810.

Masson, D. G., T. Le Bas, I. Grevemeyer, and W. Weinrebe (2008), Flank collapse and large-scale landsliding in the Cape Verde Islands, off West African, *Geochem. Geophys. Geosyst.*, *9*, doi:10.1029/2008GC001983.

McDougall, I., and H.-U. Schmincke (1976), Geochronology of Gran Canaria, Canary Islands: Age of shield building volcanism and other magmatic phases, *Bull. Volcanol.*, *40*(1), 55–77.

McGuire, B. (2010). Potential for a hazardous geospheric response to projected future climate changes, *Philos. Trans. R. Soc. A*, *368*(1919), 2317–2345.

McGuire, W. J. (1992), Changing sea levels and erupting volcanoes: Cause and effect?, *Geol. Today*, 141–144.

McGuire, W. J. (1996), Volcano instability: A review of contemporary themes, in *Volcano Instability on the Earth and Other Planets, Geol. Soc. Spec. Publ.*, vol. 110, edited by W. J. McGuire, A. P. Jones and J. Neuberg, pp. 1–24, Geol. Soc. of London, London, U. K.

McGuire, W. J. (2006), Lateral collapse and tsunamigenic potential of marine volcanoes, in *Mechanisms of Activity and Unrest at Large Calderas*, vol. 269, edited by C. Troise and D. De Natale, pp. 121–140, Blackwell, Oxford, U. K.

McGuire, W. J., A. D. Pullen and S. J. Saunders (1990), Recent dyke-induced large-scale block movement at Mount Etna and potential slope failure, *Nature*, *343*, 357–359.

McMurtry, G. M., P. Watts, G. J. Fryer, J. R. Smith, and F. Imamura (2004), Giant landslides, mega-tsunamis, and paleo-sea level in the Hawaiian Islands, *Mar. Geol.*, *203*(3-4), 219–233.

Mehl, K. W., and H.-U. Schmincke (1999), Structure and emplacement of the Pliocene Roque Nublo debris avalanche deposit, Gran Canaria, Spain, *J. Volcanol. Geotherm. Res.*, *94*(1-4), 105–134.

Miller, K. G., M. A. Kominz, J. V. Browning, J. D. Wright, G. S. Mountain, M. E. Katz, P. J. Sugarman, B. S. Cramer, N. Christie-Blick, and S. F. Pekar (2005), The Phanerozoic record of global sea-level change, *Science*, *310*(5752), 1293–1298.

Moore, J. G., D. A. Clague, R. T. Holcomb, P. W. Lipman, W. R. Normark, and M. E. Torresan (1989), Prodigious submarine landslides on the Hawaiian Ridge, *J. Geophys. Res.*, *94*(B12), 17, 465–417.

Moore, J. G., W. R. Normark, and R. T. Holcomb (1994), Giant Hawaiian landslides, *Annu. Rev. Earth Planet. Sci.*, *22*, 119–144, doi:10.1146/annurev.ea.22.050194.001003.

Mosar, J., Lewis, G., and T. Torsvik (2002), North Atlantic sea-floor spreading rates: Implications for the Tertiary development of inversion structures of the Norwegian-Greenland Sea, *J. Geol. Soc.*, *159*, 503–515, doi:10.1144/0016–764901-135.

Murray, J. B., and B. Voight (1996), Slope stability and eruption prediction on the eastern flank of Mount Etna, in *Volcano Instability on the Earth and Other Planets, Geol. Soc. Spec. Publ.*, vol. 110, edited by W. J. McGuire, A. P. Jones and J. Neuberg, pp. 111–114, Geol. Soc. of London, London, U. K.

Murty, T. S. (2003), Tsunami wave height dependence on landslide volume, *Pure Appl. Geophys.*, *160*(2003), 2147–2153.

Nelder, J. A., and R. W. M. Wedderburn (1972), Generalized linear models, *J. Royal Statistical Soc., Series A*, *135*, 370–384.

Oehler, J. F., P. Labazuy, and J. F. Lénat (2004), Recurrence of major flank landslides during the last 2Ma history of Réunion Island, *Bull. Volcanol.*, *66*(7), 585–598.

Oehler, J. F., J. F. Lénat, and P. Labazuy (2008), Growth and collapse of the Réunion Island volcanoes, *Bull. Volcanol.*, *70*(6), 717–742.

Paris, R., H. Guillou, J. C. Carracedo, and F. J. Perez-Torrado (2005), Volcanic and morphological evolution of La Gomera (Canary Islands), based on new K-Ar ages and magnetic stratigraphy: Implications for oceanic island evolution, *J. Geol. Soc.*, *162*, 501–512.

Parzen, E. (1962), On estimation of a probability density function and mode, *Ann. Math. Stat.*, *33*(3), 1065–1076.

Pearce, T. J., and I. Jarvis (1992), Composition and provenance of turbidite sands: Late quaternary, Madeira Abyssal Plain, *Mar. Geol.*, *109*, 21–51.

Pearce, T. J., and I. Jarvis (1995), High-resolution chemostratigraphy of Quaternary distal turbidites: A case study of new methods for the analysis and correlation of barren sequences, in *Non-Biostratigraphical Methods of Dating and Correlation, Geol. Soc. Spec. Publ.*, vol. 89, edited by R. E. Dunay, and E. A. Hailwood, pp. 107–143, Geol. Soc. of London, London, U. K.

Peduzzi, P., J. Concato, A. R. Feinstein, and T. R. Holford (1995), Importance of events per independent variable in proportional hazards regression analysis II. Accuracy and precision of regression estimates, *J. Clin. Epidemiol.*, *48*(12), 1503–1510.

Rothwell, R. G., B. Alibes, and P. P. E. Weaver (1998), Seismic facies of the Madeira Abyssal Plain: A correlation between seismic reflection profile and borehole data, *Proc. Ocean Drill. Prog. Sci. Results*, *157*, 473–498.

Schmincke, H.-U., and B. Segschneider (1998), Shallow submarine to emergent basaltic shield volcanism of Gran Canaria: Evidence from drilling into the volcanic apron, in *Proceedings of Ocean Drilling Program, Scientific Results*, vol. 157, edited by P. P. E. Weaver et al., pp. 141–181, Ocean Drill. Program, College Station, Tex.

Schmincke, H. U., and M. Sumita (1998), Volcanic evolution of Gran Canaria reconstructed from apron sediments: Synthesis of VICAP Project Drilling, in *Proceedings of the Ocean Drilling Program, Scientific Results*, vol. 157, edited by P. P. E. Weaver et al., p. 443, College Station, Tex.

Schmincke, H.-U., and U. von Rad (1979), Neogene evolution of Canary Island volcanism inferred from ash layers and volcaniclastic sandstones of DSDP Site 397 (Leg 47), *Deep Sea Drill. Proj. Init. Rep.*, *47*, 703–725.

Sclater, J. G., and P. A. F. Christie (1980), Continental stretching: An explanation of the post-Cretaceous subsidence of the Central North Sea Basin, *J. Geophys. Res.*, *85*(B7), 3711–3739.

Shipboard Scientific Party (1995a), Site 950, in *Proceedings of Ocean Drilling Program, Initial Reports*, vol. 157, H.-U. Schmincke et al., pp. 51–104, Ocean Drill. Program, College Station, Tex., doi:10.2973/odp.proc.ir.157.104.1995.

Shipboard Scientific Party (1995b), Site 951, in *Proceedings of Ocean Drilling Program, Initial Reports*, vol. 157, edited by H.-U. Schmincke et al., pp. 51–104, Ocean Drill. Program, College Station, Tex., doi:10.2973/odp.proc.ir.157.104.1995.

Shipboard Scientific Party (1995c), Site 952, in *Proceedings of Ocean Drilling Program, Initial Reports*, vol. 157, edited by H.-U. Schmincke et al., pp. 51–104, Ocean Drill. Program, College Station, Tex., doi:10.2973/odp.proc.ir.157.104.1995.
Siebert, L. (1984), Large volcanic debris avalanches: Characteristics of source areas, deposits, and associated eruptions, *J. Volcanol. Geotherm. Res.*, *22*(3-4), 163–197.
Siebert, L., H. Glicken, and U. Tadahide (1987), Volcanic hazards from Bezymianny- and Bandai-type eruptions, *Bull. Volcanol. 49*(1), 435–459.
Smith, T., Smith, B, Ryan and Ryan, M. A. K. (2003), Survival analysis using Cox Proportional Hazards Modelling for single and multiple event time data, paper presented at SUGI 28 SAS Users Group International Proceedings 2003 on Statistics and Data Analysis, Seattle, Wash.
Stevenson, C. J., P. J. Talling, R. B. Wynn, D. G. Masson, J. E. Hunt, M. Frenz, A. Akhmetzhanhov, and B. T. Cronin (2013), The flows that left no trace: Very large-volume turbidity currents that bypassed sediment through submarine channels without eroding the sea floor, *Mar. Pet. Geol.*, *41*, 186–205, doi:10.1016/j.marpetgeo.2012.008.
Stillman, C. J. (1999), Giant Miocene landslides and the evolution of Fuerteventura, Canary Islands, *J. Volcanol. Geotherm. Res.*, *94*(1-4), 89–104.
Tappin, D. R. (2010), Submarine mass failures as tsunami sources: Their climate control. *Philos. Trans. R. Soc. A*, *368*(1919), 2417–2434.
Tappin, D. R., P. Watts, G. M. McMurtry, Y. Lafoy, and T. Matsumoto (2001), The Sissano, Papua New Guinea tsunami of July, 1998: Offshore evidence on the source mechanism, *Mar. Geol.*, *175*, 1–24.
Thirlwall, M. F., B. S. Singer, and G. F. Marriner (2000), ^{39}Ar-^{40}Ar ages and geochemistry of the basaltic shield stage of Tenerife, Canary Islands, Spain, *J. Volcanol. Geotherm. Res.*, *103*(1-4), 247–297, doi:10.1016/S0377-0273(00)00227-4.
Tinti, S., E. Bortolucci and A. Armigliato (1999), Numerical simulation of the landslide-induced tsunami of 1988 on Vulcano, *Bull. Volcanol.*, *61*(1-2), 121–137, doi:10.1007/s004450050267.
Tinti, S., E. Bortoluci, and C. Romagnoli (2000), Computer simulations of tsunamis due to sector collapse at Stromboli, Italy, *J. Volcanol. Geotherm. Res.*, *96*(1-2), 103–128, doi:10.1016/S0377-0273(99)00138-9.
Totland, M., and K. Jarvis (1997), Assessment of Dowex 1-X8-based anion-exchange procedures for the separation and determination of ruthenium, rhodium, palladium, iridium, platinum and gold in geological samples by inductively coupled plasma mass spectrometry, *Analyst*, *122*(1), 19–26.
Turner, A. K., and R. L. Schuster (1996), Landslides: Investigation and mitigation, *Trans. Res. Board Spec. Rep.*, 247, Natl. Acad. Press, Washington, D. C.
Urgeles, R., M. Canals, J. Baraza, B. Alonso, and D. G. Masson (1997), The laste major megalandslides of the Canary Islands: The El Golfo debris avalanche and the Canary Debris Flow, west Hierro Island, *J. Geophys. Res.*, *102*(20), 305–320.
Urgeles, R., D. G. Masson, M. Canals, A. B. Watts, and T. P. Le Bas (1999), Recurrent large-scale landsliding on the west flank of La Palma, Canary Islands, *J. Geophys. Res.*, *104*(B11), 25,331–25,348.
Urgeles, R., M. Canals, and D. G. Masson (2001), Flank stability and processes off the western Canary Islands: A review from El Hierro and La Palma, *Sci. Mar.*, *65*, 21–31.
Van den Bogaard, P., and H.-U. Schmincke (1998), ^{40}Ar/^{39}Ar of Pliocene-Pleistocene fallout tephra layers and volcaniclastic deposits in the sedimentary aprons of Gran Canaria and Tenerife (Sites 953, 954, and 956), in *Proceedings of Ocean Drilling Program, Scientific Results*, vol. 157, edited by P. P. E. Weaver et al., pp. 329–341, Ocean Drill. Program, College Station, Tex.
Van Hinte, J. E. (1978), Geohistory analysis–application of micropaleontology in exploration geology, *AAPG Bull.*, *62*, 201–222.
Vittinghoff, E., and C. E. McCulloch (2007), Relaxing the rule of ten events per variable in logistic and Cox regression, *Am. J. Epidemiol*, *165*(6), 710.
Voight, B., and D. Elsworth (1997), Failure of volcano slopes, *Geotechnique*, *47*(1), 1–31.
Voight, B., H. Glicken, R. J. Janda, and P. M. Douglass (1981), Catastrophic rockslide-avalanche of May 18, in *The 1980 Eruptions of Mount St Helens, U.S. Geol. Prof. Pap. 1250*, edited by P. W. Lipman and D. R. Mullineaux, pp. 347–378, U.S. Geological Survey, USA.
Wallis, J. R., and N. C. Matala (1970), Small sample properties of H and K—Estimators of the Hurst coefficient h, *Water Resour. Res.*, *6*(6), 1583–1594.
Walter, T., and H.-U. Schmincke (2002), Rifting, recurrent landsliding and Miocene structural reorganisation of NW-Tenerife (Canary Islands), *Int. J. Earth Sci.*, *91*(4), 615–628, doi:10.1007/s00531-001-0245-8.
Walter, T. R., V. R. Troll, B. Cailleau, A. Belousov, H.-U. Schmincke, F. Amelung, and P. Vd Bogaard (2005), Rift zone reorganization through flank instability in ocean island volcanoes: An example from Tenerife, Canary Islands, *Bull. Volcanol.*, *67*(4), 281–291.
Ward, S. N., and S. J. Day (2003), Ritter Island Volcano: Lateral collapse and tsunami of 1888, *Geophys. J. Int.*, *154*(3), 891–902.
Watt, S. F. L., et al. (2012), Combinations of volcanic-flank and seafloor-sediment failure offshore Montserrat, and their implications for tsunami generation, *Earth Planet. Sci. Lett.*, *319*, 228–240.
Watts, A. B., and D. G. Masson (1995), A giant landslide on the north flank of Tenerife, Canary Islands, *J. Geophys. Res.*, *100*(B12), 24,487–24,498, doi:10.1029/95JB02630.
Watts, A. B., and D. G. Masson (1998), Reply to comment on: A giant land-slide on the northern flank of Tenerife, Canary Islands, by A. B. Watts and D. G. Masson, *J. Geophys. Res.*, *103*(B5), 9948–9951.
Watts, A. B., and D. G. Masson (2001), New sonar evidence for recent catastrophic collapses of the north flank of Tenerife, Canary Islands, *Bull. Volcanol.*, *63*, 8–19, doi:10.1007/s004450000119.
Weaver, P. P. E. (1994), Determination of turbidity current erosional characteristics from reworked coccolith assemblages, Canary Basin, north-east Atlantic, *Sedimentology*, *4*(5), 1025–1038.
Weaver, P. P. E. (2003), Northwest Africa continental margin: History of sediment accumulation, landslide deposits, and hiatuses as revealed by drilling the Madeira Abyssal Plain, *Paleoceanography*, *18*(1), 1009, doi:10.1029/2002PA000758.
Weaver, P. P. E., and A. Kuijpers (1983), Climatic control of turbidite deposition on the Madeira Abyssal Plain, *Nature*, *306*, 360–363.
Weaver, P. P. E., and J. Thomson (1993), Calculating erosion by deep-sea turbidity currents during initiation and flow, *Nature*, *364*(6433), 136–138.
Weaver, P. P. E., R. G. Rothwell, J. Ebbing, D. Gunn, and P. M. Hunter (1992), Correlation, frequency of emplacement and source directions of megaturbidites on the Madeira Abyssal Plain, *Mar. Geol.*, *109*, 1–20.
Weaver, P. P. E., I. Jarvis, S. M. Lebreiro, B. Alibes, J. Baraza, R. Howe, and R. G. Rothwell (1998), Neogene turbidite sequence on the Madeira Abyssal Plain: Basin filling and diagenesis in the deep ocean, *Proc. Ocean Drill. Program Sci. Results*, *157*, 619–634.
Wynn, R. B., and D. G. Masson (2003), Canary island landslides and tsunami generation: Can we use turbidite deposits to interpret landslide processes, in *First International Symposium on Submarine Mass Movements and Their Consequences, Adv. Nat. and Technol. Hazards Research*, vol. 19, edited by J. Locat and J. Mienert, pp. 325–332. Kluwer Acad., Dordrecht, Netherlands.
Wynn, R. B., D. G. Masson, D. A. V. Stow, and P. P. E. Weaver (2000), The Northwest African slope apron: A modern analogue for deep-water systems with complex seafloor topography, *Mar. Pet. Geol.*, *17*, 253–265.
Wynn, R. B., P. P. E. Weaver, D. A. V. Stow, and D. G. Masson (2002), Turbidite depositional architecture across three interconnected deep-water basins on the northwest African margin, *Sedimentology*, *49*, 1441–1462, doi:10.1046/j.1365–3091.2002.00471.x.

